

# Excess iron stress reduces root tip zone growth through nitric oxide-mediated repression of potassium homeostasis in *Arabidopsis*

Lin Zhang<sup>1,2\*</sup>, Guangjie Li<sup>1\*</sup>, Meng Wang<sup>1</sup>, Dongwei Di<sup>1</sup>, Li Sun<sup>1</sup>, Herbert J. Kronzucker<sup>3</sup> and Weiming Shi<sup>1</sup>

<sup>1</sup>State Key Laboratory of Soil and Sustainable Agriculture, Institute of Soil Science, Chinese Academy of Sciences, No. 71 East Beijing Road, Nanjing 210008, China; <sup>2</sup>University of the Chinese Academy of Sciences, No. 19(A) Yuquan Road, Shijingshan District, Beijing 100049, China; <sup>3</sup>School of BioSciences, The University of Melbourne, Parkville, Vic. 3010, Australia

Authors for correspondence:

Guangjie Li  
Tel: +86 02586881578  
Email: gili@issas.ac.cn

Weiming Shi  
Tel: +86 02586881566  
Email: wmsi@issas.ac.cn

Received: 15 January 2018

Accepted: 9 March 2018

New Phytologist (2018) 219: 259–274  
doi: 10.1111/nph.15157

**Key words:** *Arabidopsis*, Fe excess, K<sup>+</sup> efflux, K<sup>+</sup> homeostasis, nitric oxide, primary root growth, root tip zone, SNO1/SOS4.

## Summary

- The root tip zone is regarded as the principal action site for iron (Fe) toxicity and is more sensitive than other root zones, but the mechanism underpinning this remains largely unknown.
- We explored the mechanism underpinning the higher sensitivity at the *Arabidopsis* root tip and elucidated the role of nitric oxide (NO) using NO-related mutants and pharmacological methods.
- Higher Fe sensitivity of the root tip is associated with reduced potassium (K<sup>+</sup>) retention. NO in root tips is increased significantly above levels elsewhere in the root and is involved in the arrest of primary root tip zone growth under excess Fe, at least in part related to NO-induced K<sup>+</sup> loss via SNO1 (*sensitive to nitric oxide 1*)/SOS4 (*salt overly sensitive 4*) and reduced root tip zone cell viability. Moreover, ethylene can antagonize excess Fe-inhibited root growth and K<sup>+</sup> efflux, in part by the control of root tip NO levels.
- We conclude that excess Fe attenuates root growth by effecting an increase in root tip zone NO, and that this attenuation is related to NO-mediated alterations in K<sup>+</sup> homeostasis, partly via SNO1/SOS4.

## Introduction

Iron (Fe) is an essential element, but is also toxic to plants when present at elevated levels, as frequently occurs in soils of low pH and oxygen tension (Connolly & Guerinot, 2002; Becker & Asch, 2005). Plants grown in soil containing excess Fe exhibit visible symptoms of toxicity, including biomass reduction, root growth inhibition, Fe plaques in roots, leaf bronzing and necrosis. Although physiological and molecular responses to Fe deficiency have been well documented, plant responses to Fe toxicity and Fe toxicity-related mechanisms have received less attention.

The root is the first organ to sense excess Fe, and Fe toxicity plays a direct role in the modulation of root system architecture (Li *et al.*, 2016b; Onaga *et al.*, 2016). A rapid response of root tips to their changing surroundings is crucial if root development is to proceed under adverse soil conditions. Recent studies have shown that the root tip is more sensitive than other root zones to Fe, but the mechanisms underpinning this are still largely unknown (Zhang *et al.*, 2011, 2012; Li *et al.*, 2015a,b). The elucidation of the mechanisms of how root tips respond to Fe toxicity will greatly help to improve our understanding of the

adaptation and acclimation of root system architecture to metal stresses.

Plant hormones and other molecules are important intermediary signaling compounds that function downstream of environmental stimuli. Several messenger molecules, such as ethylene and reactive oxygen species (ROS), are involved in the mediation of Fe excess-dependent changes in root growth. Fe excess can increase H<sub>2</sub>O<sub>2</sub> production in the tip zone and arrest primary root growth (Reyt *et al.*, 2015). Meanwhile, ethylene evolution is enhanced by the upregulation of the expression of 1-aminocyclopropane-1-carboxylic acid synthase (ACS) genes in the root tip and can protect root growth under Fe toxicity (Li *et al.*, 2015b). Recent research has unveiled NO as a critical component in plant acclimation responses to a variety of stresses, such as cadmium (Cd), copper (Cu) and aluminum (Al) stress (Neill *et al.*, 2003; Crawford & Guo, 2005; Tian *et al.*, 2007; Peto *et al.*, 2013; Alemayehu *et al.*, 2015). Under Fe scarcity, NO increases in the root and can affect Fe uptake from the culture environment (Pagnussat *et al.*, 2002; Graziano & Lamattina, 2007). Similarly, NO production has been reported to increase under Fe overload (Arnaud *et al.*, 2006; Touraine *et al.*, 2012). Thus, it could be predicted that there may be links between NO and the Fe toxicity response in plants. However, there has been no detailed study to evaluate the role of NO in the Fe toxicity

\*These authors contributed equally to this work.

response in plant development, and especially not in relation to primary root growth.

A number of studies have shown that intracellular potassium ( $K^+$ ) participates in many defense-related processes, and that various abiotic and biotic stresses induce  $K^+$  efflux from root cells (Demidchik *et al.*, 2003, 2010). In most cases, this  $K^+$  efflux is mediated by  $K^+$ -selective channels, nonselective cation channels (NSCCs) and annexins (reviewed in Demidchik, 2014). The guard cell outward-rectifying  $K^+$  channel (GORK) *GORK1* is well known to conduct large outwardly directed  $K^+$  currents from root cells in response to copper ascorbate and/or NaCl, and NaCl-activated  $K^+$  efflux from roots is significantly decreased in the *gork1-1* mutant (Demidchik *et al.*, 2010; Demidchik, 2014). NSCCs belong to a variety, and as yet to be solidly identified, gene families (e.g. cyclic nucleotide-gated channel (CNGC) gene families contain 20 genes in *Arabidopsis*, glutamate receptor (GLR) gene families contain 20 genes in *Arabidopsis*) forming a group with a cryptic molecular identity and diverse functional characteristics (Demidchik & Maathuis, 2007; Kronzucker & Britto, 2011). The big challenge in studies of plasma membrane-resident NSCCs is the persistent lack of knowledge of the encoding genes and the fact that single loss-of-function mutations do not result in clear phenotypes (Pottosin & Dobrovinskaya, 2014). Under Fe toxicity, a significant loss of plant tissue  $K^+$  level has been noted (Li *et al.*, 2001, 2015b, 2016a), but the morphological and physiological mechanisms of root  $K^+$  homeostasis under Fe excess have not been identified. A recent study showed that ethylene can maintain root  $K^+$  status by regulating  $K^+$  uptake to support root growth under Fe toxicity (Li *et al.*, 2015b). In addition, the possibility that NO contributes to modulate  $K^+$  accumulation by plants has been advanced recently (Simontacchi *et al.*, 2015). The *SNO1* (*sensitive to nitric oxide 1*)/*SOS4* (*salt overly sensitive 4*) gene encoding a pyridoxal kinase has been identified recently to play a critical role in NO-mediated root  $K^+$  homeostasis (Shi *et al.*, 2002; Xia *et al.*, 2014). Xia *et al.* (2014) demonstrated that enhanced NO increases the accumulation of pyridoxal-5'-phosphate (PLP), which, in turn, represses  $K^+$  uptake in *Arabidopsis* roots, and NO-triggered PLP accumulation mainly occurs through NO-induced SNO1/SOS4 enzyme activity. Although ethylene and NO signals have been implicated as important for root  $K^+$  homeostasis, it remains largely unknown how ethylene and NO are involved in the response of root  $K^+$  homeostasis to excess Fe.

In this study, we employed *Arabidopsis Columbia-0* (*Col-0*) and NO- and ethylene-related mutants to explore the possible mechanism underpinning the higher sensitivity to Fe toxicity of the root tip zone, and to elucidate the roles of NO and ethylene. The potential mechanisms involved in the stress response to excess Fe are discussed.

## Materials and Methods

### Plant materials and growth conditions

Seedlings of the following lines were used in this study: *Arabidopsis thaliana* (L.) Heynh. ecotype *Columbia-0* (*Col-0*); the

mutants *nox1* (*nitric oxide overproducer1*), *gsnor1* (*S*-nitrosogluthione (GSNO) reductase1), *sno1/sos4*, *noa1* (NO Associated1), *pin2-1*, *pin3-5*, *tir1-1*, *pin1-1*, *axr2-1*, *axr3-3* (*Arabidopsis* Biological Resource Center, Supporting Information Table S1) and *eto2-1*, and the *EIN3 binding site (EBS):b-Glucuronidase (GUS)*, *Direct Repeat 5 (DR5):GUS*, *ACS7:GUS* and *DR5:Green Fluorescent Protein (GFP)* transgenic lines, were in a *Col-0* background; the *gork1* mutant was in a *Wassilewskija* (*WS*) background. Seeds were surface sterilized and cold treated at 4°C for 48 h before being sown on standard growth medium. The standard growth medium has been described previously (Li *et al.*, 2013), and was as follows: 2 mM  $KH_2PO_4$ , 5 mM  $NaNO_3$ , 2 mM  $MgSO_4$ , 1 mM  $CaCl_2$ , 50  $\mu$ M Fe-EDTA, 50  $\mu$ M  $H_3BO_3$ , 12  $\mu$ M  $MnSO_4$ , 1  $\mu$ M  $ZnCl_2$ , 1  $\mu$ M  $CuSO_4$ , 0.2  $\mu$ M  $Na_2MoO_4$ , 1% sucrose, 0.5 g/l MES and 0.8% agar (adjusted to pH 5.7 with 1 M NaOH). The day of sowing was considered as day 0. Seedlings were grown vertically on the surface of the culture plates in a growth chamber set to a 16 h : 8 h, light : dark photoperiod, an irradiance of 100  $\mu$ mol  $m^{-2} s^{-1}$  and a temperature of  $23 \pm 1^\circ C$ . Excess Fe was supplied as Fe-EDTA ( $FeSO_4 \cdot 7H_2O$  plus EDTA, 1 : 1 molar ratio). The pH was set to 5.3 based on our previous report (Li *et al.*, 2015b). To study the effect of exogenous 2-(4-carboxyphenyl)-4,4,5,5-tetramethylimidazole-1-oxyl-3-oxide (cPTIO), sodium nitroprusside (SNP), aminoethoxyvinylglycine (AVG), NG-nitro-L-arginine methyl ester (L-NAME), NG-monomethyl-L-arginine (L-NMME), tetraethylammonium (TEA),  $Gd^{3+}$  and  $K^+$  (supplied as  $K_2SO_4$ ), seedlings were supplemented with varying concentrations of Fe-EDTA plus the indicated concentrations of the added compounds. All chemicals were obtained from Sigma-Aldrich.

### Localized Fe supply experiments

Localized excess Fe treatments are shown in Fig. S1, as described in our previous report (Li *et al.*, 2015a). Briefly, for 'root tip-supplied' plants, segmented agar plates were separated into upper and lower parts with a 3-mm air gap, using movable glass strips, 3 mm in width. Growth medium was poured into the upper part, the excess Fe-EDTA medium was poured into the bottom part, and only the primary root tip of the seedlings (*c.* 2 mm) was in contact with the excess Fe-EDTA medium. For 'root hair zone-supplied Fe' plants, growth medium was poured into the bottom part, excess Fe-EDTA medium was poured into the upper part, and only the shoot and primary root hair zone of the seedlings were in contact with the excess Fe-EDTA medium. Treatment was for the times indicated.

### Root measurements

Roots on the agar surface were sampled. The lengths of the primary roots of individual seedlings were measured directly with IMAGEJ software (National Institutes of Health; <http://rsb.info.nih.gov/ij>) from digital images captured with a Canon G7 camera. Primary root elongation was defined as the length of the root parts newly grown after treatment. Measurements were made of the length from the root cap to the first root hair.

## Microscopy and image and mineral analysis

The Fe-specific Perls staining and diaminobenzidine (DAB) intensification were adapted from Roschztardt *et al.* (2009). Localization of Fe was observed and imaged using an Olympus BX51 microscope equipped with differential interference contrast (DIC) optics and an Olympus DP71 camera. Histochemical analysis of GUS reporter enzyme activity was performed as described elsewhere (Weigel & Glazebrook, 2002). Trypan blue (TB) staining was used to assess the level of cell death in the root tips under excess Fe according to the method of Duan *et al.* (2010) with some modifications. The *DR5::GFP* reporter was analyzed using a Zeiss LSM710 confocal microscope, and image analysis was performed using ZEISS 2009 software (Carl Zeiss AG, Jena, Germany). NO and ROS were visualized using the NO-specific fluorescent probe 3-amino,4-aminomethyl-2',7'-difluorescein diacetate (5  $\mu$ M) and the ROS fluorescent probe 5-(and-6)-chloromethyl-2',7'-dichlorodihydrofluorescein diacetate, acetyl ester (25  $\mu$ M), respectively, according to the method of Wang *et al.* (2014) with some modifications. Asante Potassium Green-2 (APG-2; TEFLabs, Austin, TX, USA) and CoroNa Green acetoxymethyl (AM) ester (Invitrogen, Eugene, OR, USA) were employed to measure  $K^+$  and  $Na^+$  concentrations according to Wang *et al.* (2016); 20  $\mu$ M APG-2 and CoroNa Green were added to measuring buffers, respectively ( $K^+$ : 5 mM NaCl, 5 mM  $Ca^{2+}$ -MES, pH 6.1;  $Na^+$ : 10 mM KCl, 5 mM  $Ca^{2+}$ -MES, pH 6.1) and incubated with the *Arabidopsis* seedlings for 3 h in the dark at room temperature. The fluorescence intensity of NO, APG-2, CoroNa Green and ROS was determined by calculating the relative contribution of the green channel using the values of the RGB color model as measured in PHOTOSHOP 7.0 (Adobe Systems Inc., San Jose, CA, USA), according to Teerawanichpan *et al.* (2007). All staining and image analysis procedures were repeated at least twice, and the results shown are from one of two representative experiments. For mineral analyses, samples were obtained from root tip sections (*c.* 1–2 mm) from both control and excess Fe treatments. The samples (0.5–1.0 mg) were digested with 0.25 ml of concentrated  $HNO_3$  at 110°C for 2 h according to Ward *et al.* (2008) and analyzed on an Inductively Coupled Plasma Mass Spectrometry (Agilent, Santa Clara, CA, USA).

## Enzyme activity analyses of SNO1/SOS4

The activity of SNO1/SOS4 was measured using a colorimetric procedure, according to the protocols described by Xia *et al.* (2014). Briefly, 0.5 ml of crude extract (containing 1–7 mg of total protein) was used in a buffer containing 0.2 mM pyridoxal, 0.2 mM ATP, 0.1 mM  $ZnCl_2$  and 70 mM  $K_3PO_4$ . After 1 h of incubation at 37°C, reactions were stopped by the addition of 50 mL of chilled 50% trichloroacetic acid (TCA) (w/v). Protein was pelleted by centrifugation (1500 g) at 4°C for 10 min, and the supernatant was transferred to a clean tube. After the addition of 2% phenylhydrazine (in 10 N  $H_2SO_4$ ) and incubation on ice for 30 min, PLP formation was measured based on the absorbance at 410 nm. Each reaction was repeated three times.

## Measurement of net $K^+$ flux with the SIET system

Net fluxes of  $K^+$  were measured from the root apical (*c.* 500  $\mu$ m from the tip of *Col-0* roots) transition zone and the root hair (*c.* 3000  $\mu$ m from the tip of *Col-0* roots) zone non-invasively using SIET (scanning ion-selective electrode technique, SIET system BIO-003A; Younger USA Science and Technology Corp.; Applicable Electronics Inc.; Science Wares Inc., Falmouth, MA, USA). The principle of this method and the instrument are detailed in Li *et al.* (2010) and Shabala *et al.* (2016). *Arabidopsis* seedlings were grown in a Petri dish for 7 d. For pretreatments, plants were pretreated with mock solution plus the indicated concentrations of cPTIO, SNP, TEA,  $Gd^{3+}$ , AVG, PLP and  $K^+$  for 2 h. After the specified pretreatment duration, the pretreatment solution was withdrawn and the measuring solution was introduced. Net ion fluxes were first measured in the basal medium to ensure steady initial values, and then 10 mM stock solution of Fe-EDTA was applied to reach a final Fe concentration of 300  $\mu$ M. Transient recordings of the flux kinetics of  $K^+$  were measured for specified times. All measurements of net  $K^+$  fluxes were carried out at Xuyue Science and Technology Co. Ltd. (Beijing, China).

## Statistical and graphical analyses

For all experiments, data were statistically analyzed using the SPSS 13.0 program (SPSS, Chicago, IL, USA). Details are as presented in the figure legends. Graphs were produced using ORIGIN 8.0. All graphs and images were prepared using Adobe PHOTOSHOP 7.0 (Adobe Systems Inc.).

## Results

### The root tip is the critical site in the arrest of *Arabidopsis* primary root growth under Fe toxicity

To analyze the effect of Fe toxicity on primary root growth, *Arabidopsis* seedlings were allowed to come into contact with varying concentrations of Fe-EDTA. Based on our previous report (Li *et al.*, 2015b), 50  $\mu$ M Fe was used as a control. Increased Fe concentrations significantly inhibited primary root growth (Fig. 1a). Primary root growth was also quantified at 1, 2 and 3 d after transfer. Exposure of the seedlings to excess Fe (300  $\mu$ M) resulted in an immediate arrest of root growth at the indicated time (Fig. 1b). Further results showed that Fe excess-induced root growth inhibition required that the root tip was in direct contact with external Fe (Figs S1, 1c), and the distance from the root apex to the emergence of the first root hair under Fe toxicity was reduced to *c.* 50% of that in controls (Fig. 2a,b). These results suggest that root apical tissues are more sensitive to excess Fe and are immediately growth arrested on excess Fe treatment.

To investigate whether the higher sensitivity of the root apex is associated with higher Fe accumulation than in the root hair zone, we used a sensitized, Fe-specific, histochemical procedure (Perls/DAB staining) that reports labile (nonheme)  $Fe^{3+}$  and some  $Fe^{2+}$  (Meguro *et al.*, 2007; Muller *et al.*, 2015). Under

excess Fe, the intensity of Perls/DAB was much deeper in the root hair zone compared with the tip zone (Fig. 2c). The phenomenon was also observed by the Perls method (no DAB enhancement) (Fig. S2). Thus, the arrest of root growth on exposure of the root tip to excess Fe (Figs 1c, 2a,b) may not be explained by a higher accumulation of Fe in the root tip.

Higher sensitivity of the root tip zone to Fe may be related to impaired  $K^+$  homeostasis

$K^+$  has been reported to play a critical role in the regulation of root development under Fe toxicity. We thus analyzed changes in  $K^+$  level in functionally different root zones (root hair zone and tip zone). Imaging using the APG2 fluorescing dye revealed that excess Fe led to a decline in the  $K^+$  level of the root tip zone, but no significant changes were observed in the root hair zone over the times of treatment (Fig. 2d,e). Mineral analysis using ICP-MS further showed a significant decrease in the root tip zone  $K^+$  content under excess Fe treatment (Fig. 2f). Analysis of root growth revealed localized  $K^+$  deficiency in the root tip, but not in the root hair zone, enhancing the sensitivity of root growth to Fe (Fig. S3). In addition, a slight decrease was found in root tip zone sodium (Na) staining (Fig. S4a). However, localized  $Na^+$  deficiency in the root tip zone did not significantly enhance the sensitivity of root growth to Fe toxicity (Fig. S4b). There was no significant decrease in the root tip zone calcium (Ca) and magnesium (Mg) contents over the same time of excess Fe treatment (Fig. S4c).

To examine  $K^+$  net fluxes at the root surface in response to excess Fe in functionally different *Col-0* root zones, we used SIET on *Arabidopsis* roots (Ludewig *et al.*, 2003). On excess Fe stimulation, there was a significant efflux of intracellular  $K^+$  in the tip zone (Fig. 3a). By contrast, the root hair zone (*c.* 3000  $\mu$ m from the tip of roots) showed no remarkable changes in SIET signals under the same conditions. The mean  $K^+$  effluxes under excess Fe were significantly different between the two root zones (Fig. 3b). As described above, Fe-inhibited root growth requires that the root tip come into contact with external Fe (Fig. 1c). It was

therefore important to ask whether  $K^+$  fluxes at the root apex may be changed by direct Fe contact. The addition of excess Fe to the whole root or only the root tip resulted in a massive  $K^+$  efflux in the root tip zone, whereas the mean  $K^+$  flux was similar when the whole root or only the root tip zone was exposed to excess Fe (Fig. 3c,d). When excess Fe was not supplied to the root tip, there were no significant changes in SIET signals in the root tip zone (Fig. 3c,d).

$K^+$ -selective channels and NSCCs are documented to be involved in  $K^+$  efflux from roots (Coskun *et al.*, 2010; Kronzucker & Britto, 2011; Demidchik, 2014; Shabala *et al.*, 2016). To delineate between these channels, exogenous TEA, a well-known inhibitor of  $K^+$  channel activity (Coskun *et al.*, 2010, 2013b), and  $Gd^{3+}$ , a known blocker of NSCCs (Kronzucker & Britto, 2011), were applied to *Arabidopsis* seedlings. Compared with the mock condition, Fe-induced  $K^+$  efflux was similar in TEA-pretreated seedlings. However, the  $Gd^{3+}$  application significantly decreased the Fe-induced root tip  $K^+$  efflux (Fig. 4a,b) and mildly alleviated the decrease in the rate of root growth compared with Fe treatment alone (Fig. S5a). The outwardly rectifying  $K^+$  channel *GORK1* is well known to conduct large  $K^+$  effluxes in response to Cu and Na (Demidchik *et al.*, 2010; Demidchik, 2014). However, mean  $K^+$  effluxes in the root tip zone did not show significant differences between the wild-type and the *gork1* mutant under excess Fe, and root growth was decreased in *gork1* to a similar extent as in the wild-type (Figs 4c,d, S5b).

$K^+$  deficiency resulted in severe root growth inhibition, and the root growth inhibition by excess Fe in *Col-0* was alleviated by  $K^+$  addition (Becker & Asch, 2005; Li *et al.*, 2015b; Fig. S6a).  $K^+$  addition led to increased tip zone K content, but did not affect  $K^+$  efflux at the root tip in response to excess Fe (Fig. S6b,c).

### Excess Fe affects root tip zone growth through the overaccumulation of NO

Fe overload stimulates NO accumulation (Arnaud *et al.*, 2006). Indeed, treatment with excess Fe resulted in the significant accumulation of NO in *Arabidopsis* roots (Fig. 5a,b). However, this

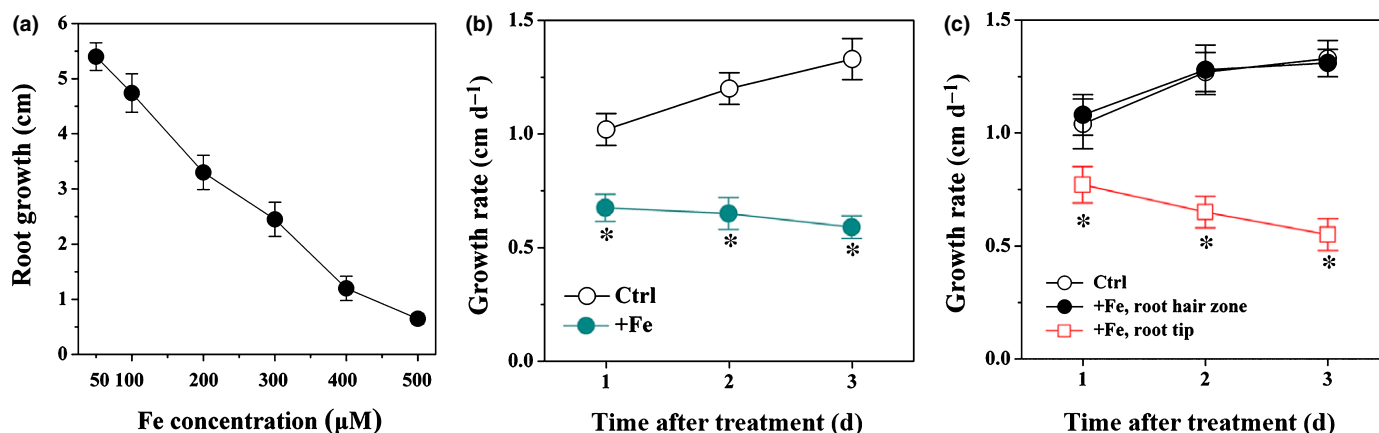


**Fig. 1** Effects of excess iron (Fe) on primary root growth in *Arabidopsis thaliana* (*Col-0*). (a) Primary root growth of 5-d-old *Col-0* exposed to serial concentrations of Fe-EDTA for 5 d. (b) Root growth rate as a function of time after treatment. Ctrl, control, 50  $\mu$ M Fe; +Fe, excess Fe, 300  $\mu$ M Fe. (c) The effect of locally supplied Fe on root growth rate as a function of time after treatment. Values shown are means  $\pm$  SD ( $n \geq 14$ ). Asterisks indicate statistically significant differences between control (Ctrl) and excess Fe treatment (+Fe) (independent samples *t*-test,  $P < 0.05$ ).



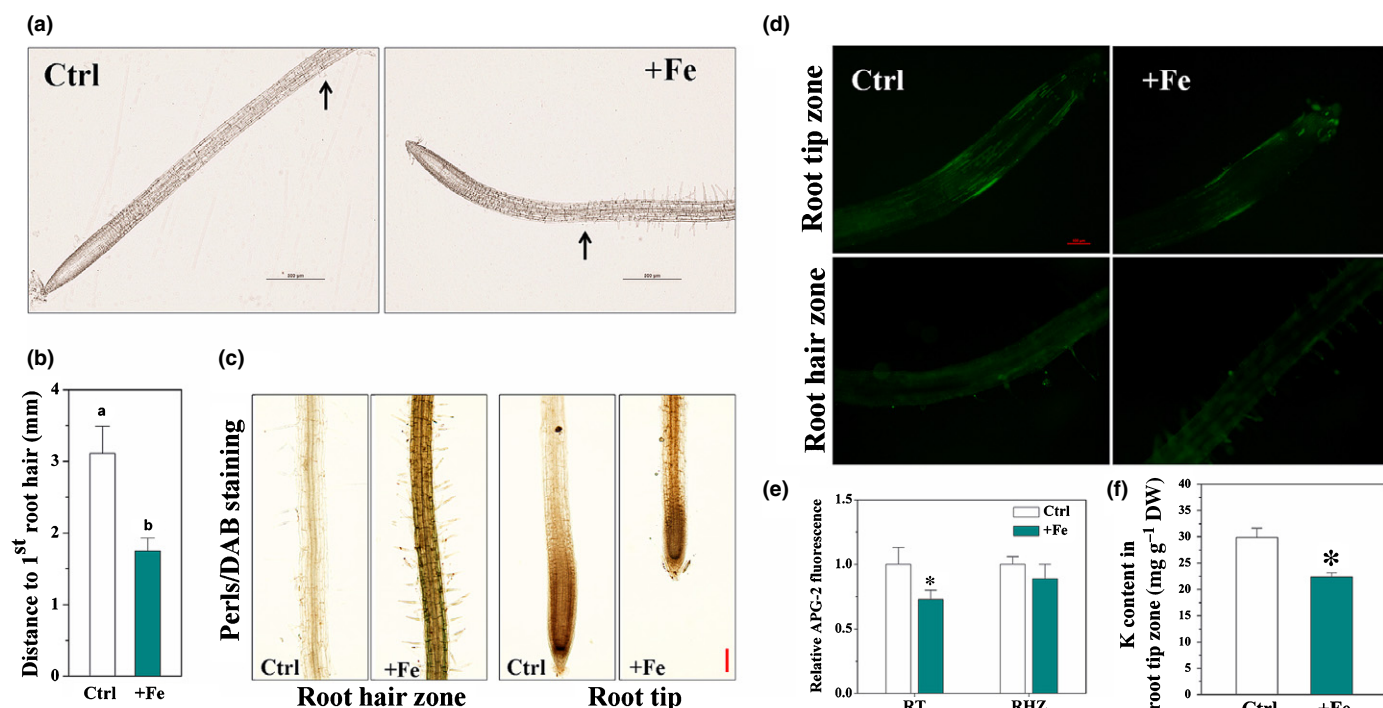


**Fig. 2** Effects of excess iron (Fe) on root Fe and K<sup>+</sup> homeostasis in control and excess Fe-treated *Arabidopsis thaliana* (Col-0) seedlings. (a) Distance from the root apex to the first root hair of the primary root. Photographs show representative seedlings treated for 3 d. Black arrows indicate the position of the first root hair. (b) The quantification of distance from the root apex to the first root hair. Asterisk denotes statistical significance (independent samples *t*-test, *n* = 20–21, *P* < 0.05). (c) Fe accumulation and distribution in primary roots. Five-day-old Col-0 seedlings exposed to excess Fe for 3 d before Perls/diaminobenzidine (DAB) staining. (d) Effect of excess Fe on K<sup>+</sup> staining in the *Arabidopsis* root hair zone and tip zone. Five-day-old Col-0 seedlings exposed to excess Fe for 3 d before staining with K<sup>+</sup> indicator (Asante Potassium Green-2, APG-2). (e) The mean relative APG-2 fluorescence intensity in the root tip (RT) and root hair zone (RHZ) of control and excess Fe-treated seedlings. The fluorescence intensity of control root tip and hair zone was set to 1. Asterisk denotes statistical significance (independent samples *t*-test, *n* = 12, *P* < 0.05). (f) Effect of Fe excess on K content in the root tip zone. Five-day-old Col-0 seedlings were transferred for 3 d to control or excess Fe before harvesting of the root tips (c. 1–2 mm) for Inductively Coupled Plasma–Mass Spectrometry measurements of K (values shown are the means ± SD of three replicates, each with three biological replicates of c. 100 root tips each; asterisk denotes statistical significance). Bars: (a) 500 µm; (c, d) 100 µm.

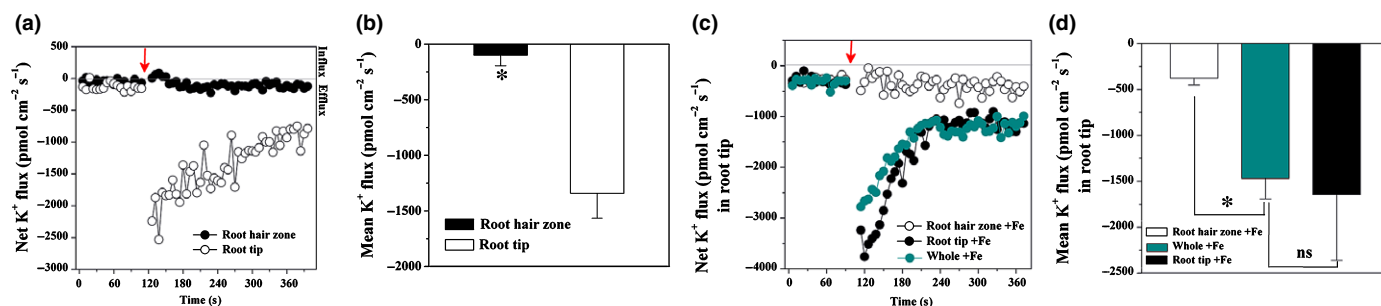


**Fig. 3** Influence of excess iron (Fe) on net plasma membrane K<sup>+</sup> fluxes of *Arabidopsis thaliana* (Col-0). (a) Net K<sup>+</sup> fluxes measured from the epidermal root cells in the root apical (c. 500 µm from the tip) transition zone and root hair (c. 3000 µm from the tip) zone of Col-0 seedlings in response to 300 µM Fe treatment (indicated by the arrow). (b) Mean values of K<sup>+</sup> fluxes from (a). Asterisk denotes statistical significance (independent samples *t*-test, *P* < 0.05). (c) The effect of locally supplied Fe on net K<sup>+</sup> fluxes in the root tip zone (indicated by the arrow). (d) Mean values of K<sup>+</sup> fluxes from (c). Asterisk denotes statistical significance (independent samples *t*-test, *P* < 0.05; ns, nonsignificant). Values shown are the means ± SD (*n* ≥ 3). Whole + Fe, whole seedlings supplied with excess Fe.

accumulation was more significant in the root tip zone (Fig. 5a, b).

To investigate the possible role of NO in Fe-induced inhibition of root growth, we first investigated the effects of cPTIO (a widely used NO scavenger) and SNP (an NO donor) on root growth under excess Fe. Application of cPTIO clearly reversed

the decrease in the rate of primary root growth and the root tip zone size compared with Fe treatment alone (Fig. 6a,b). However, application of SNP to the root tip clearly enhanced the Fe-induced inhibition of root growth (Fig. 6c). Infiltration with either L-NAME or L-NMME (inhibitors of animal NO synthase (NOS) which is also effective in plant systems) did not

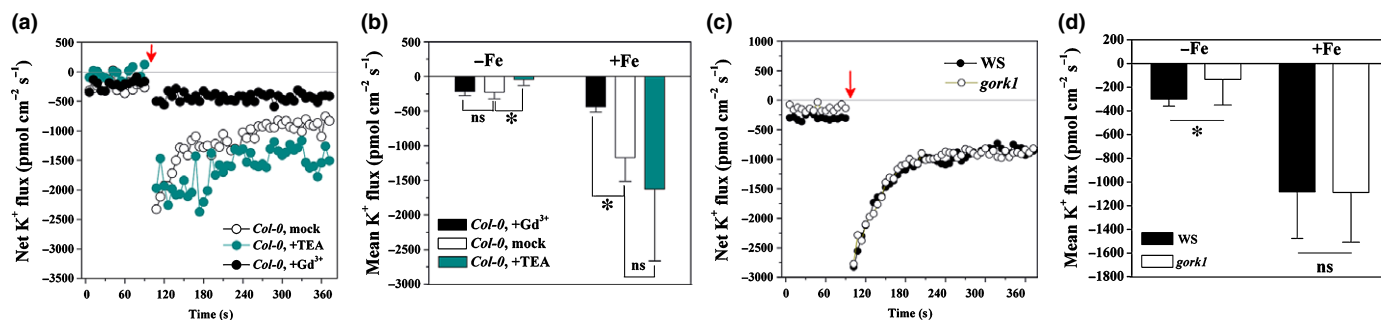


**Fig. 4** The effect of excess iron (Fe) on net plasma membrane K<sup>+</sup> efflux in the root tip zone of *Arabidopsis thaliana* *Col-0* with or without tetraethylammonium (TEA), Gd<sup>3+</sup> pretreatment, and in the *gork1* mutant. (a) Effect of TEA (10 mM) and Gd<sup>3+</sup> (50  $\mu$ M) pretreatment on net K<sup>+</sup> fluxes measured from the epidermal root cells in the *Col-0* root apical zone in response to 300  $\mu$ M Fe treatment (indicated by the arrow). (b) Mean values of K<sup>+</sup> fluxes from (a). Asterisk denotes statistical significance (independent samples *t*-test,  $n \geq 3$ ,  $P < 0.05$ ; ns, nonsignificant). (c) The net K<sup>+</sup> fluxes measured from the epidermal root cells in the *Wassilewskija* (WS) and *gork1* root apical zone in response to 300  $\mu$ M Fe treatment (indicated by the arrow). (d) Mean values of K<sup>+</sup> fluxes from (c). Asterisk denotes statistical significance (independent samples *t*-test,  $n = 8$ ,  $P < 0.05$ ; ns, nonsignificant). Values shown are the means  $\pm$  SD.

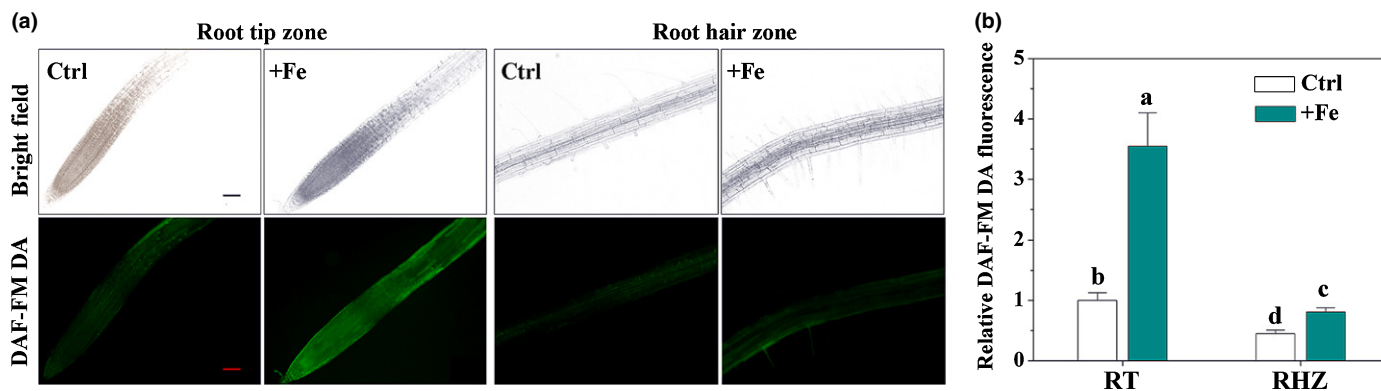


**Fig. 5** Effects of excess iron (Fe) on the production of nitric oxide (NO) in roots of *Arabidopsis thaliana* *Col-0* plants; 5-d-old *Col-0* seedlings exposed to excess Fe for 2 d. (a) The endogenous NO level in the root tip zone and root hair zone was monitored by labeling NO using the NO-specific fluorescent probe 3-amino,4-aminomethyl-2',7'-difluorescein, diacetate (DAF-FM DA) and imaged by epifluorescence microscopy. Bars, 100  $\mu$ m. (b) The mean relative DAF-FM DA fluorescence intensity in the root tip (RT) and root hair zone (RHZ) of control and excess Fe-treated seedlings. The fluorescence intensity of the control root tip zone was set to 1. Values shown are the means  $\pm$  SD ( $n = 15$ ). Different letters represent means that are statistically significantly different at the 0.05 level (one-way ANOVA with Duncan *post-hoc* test). Ctrl, control (50  $\mu$ M Fe); +Fe, excess Fe (300  $\mu$ M Fe).

significantly modify Fe-induced inhibition of primary root growth (Fig. S7a), whereas these compounds have been shown to reduce the inhibitory effect of salt treatment on root growth (Liu *et al.*, 2015; Fig. S7b). Furthermore, the root growth of the *noa1* mutant, which exhibits reduced endogenous NO levels, was also similar to *Col-0* under Fe excess (Fig. S7c). This result supports the previous finding that NOS inhibitors (L-NAME and L-NMME) and the mutation in NOA1 do not significantly affect the excess Fe-induced NO production (Touraine *et al.*, 2012).

In agreement with pharmacological studies, exposure of the NO overproduction mutants *nox1* and *gsnor1* to excess Fe concentrations led to greater inhibition of root growth than in *Col-0* (Figs 6d, S8). To ascertain that the observed primary root phenotypes were specifically caused by high Fe concentrations and not by the organic chelate, similar experiments were performed using Fe-citrate instead of Fe-EDTA (Fig. S9), and *nox1* retained higher sensitivity of root growth. The spatial response to Fe was also compared between *Col-0* and *nox1*, and a difference in Fe-inhibited root growth between the two genotypes was only found

when the root tips were exposed to excess Fe (Fig. 6e). In agreement with this, the size of the primary root tip zone was more strongly reduced in *nox1* than in *Col-0* when Fe was supplied in a localized manner to the root tip (Fig. 6f). Fe excess has been documented to be associated with enhanced throughput through Fenton reactions. We also tested the response of *nox1* root growth to excess Cu, which is also associated with Fenton reactions. However, *nox1* displayed increased root growth tolerance relative to *Col-0* under Cu excess (Fig. S10).

Auxin has been suggested to be involved in root growth under several stresses (Giehl *et al.*, 2012; Yuan *et al.*, 2013), and thus was examined here. Although the level of the *DR5::GUS* reporter gene in the root apex of the *wei7-2* mutant, in which auxin biosynthesis is impaired (Yang *et al.*, 2014), was markedly reduced compared with that in *Col-0* (Fig. S11a,b), Fe had a similar impact on root growth inhibition in both genotypes. Analysis of the response of auxin transport and signaling mutants showed that root growth was decreased in auxin transport mutants (*pin1-1*, *pin3-5*) and in signaling mutants (*tir1-1*, *axr2-1*, *axr3-3*) to a

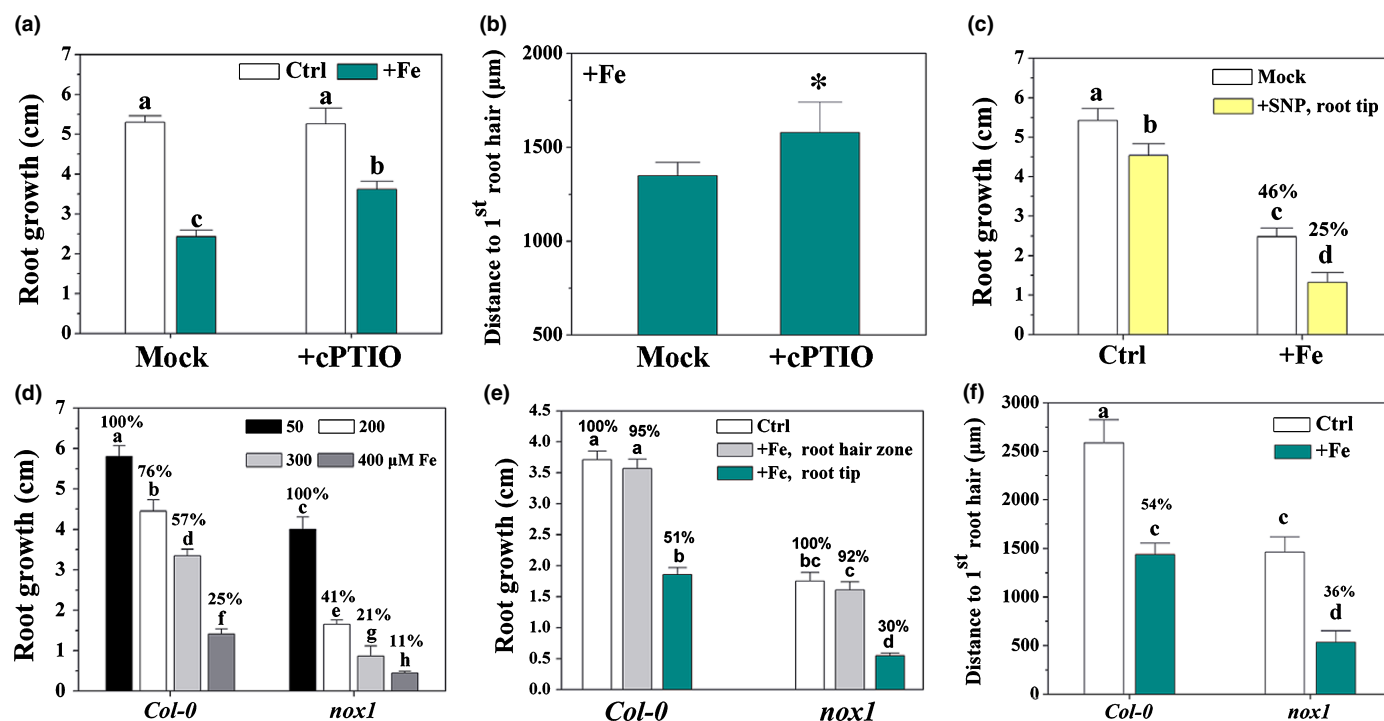


**Fig. 6** Effects of nitric oxide (NO) on excess iron (Fe)-mediated primary root growth in *Arabidopsis thaliana*. (a) Effect of NO scavenger 2-(4-carboxyphenyl)-4,4,5,5-tetramethylimidazoline-1-oxyl-3-oxide (cPTIO) (100  $\mu$ M) on the primary root growth of *Col-0* seedlings grown in control (Ctrl) and 300  $\mu$ M Fe (+Fe) medium. Five-day-old *Col-0* seedlings exposed to excess Fe for 5 d. (b) Distance from the root apex to the first root hair of the primary root. Asterisk indicates statistically significant difference between mock and treatment under excess Fe (independent samples *t*-test,  $P < 0.05$ ). (c) Effect of the NO donor sodium nitroprusside (SNP) (15  $\mu$ M) on the primary root growth of *Col-0* seedlings. Five-day-old *Col-0* exposed to excess Fe for 3 d. (d) Effect of excess Fe on the primary root growth of *Col-0* and the NO overproduction mutant *nox1*. *Col-0* and *nox1* seedlings exposed to excess Fe for 5 d. (e) Effect of locally supplied Fe on the root growth of *Col-0* and *nox1*. *Col-0* and *nox1* seedlings exposed to excess Fe for 3 d. (f) Distance from the root apex to the first root hair of the primary root. Values shown are the means  $\pm$  SD ( $n \geq 10$ ). Different letters represent means that are statistically significantly different at the 0.05 level (one-way ANOVA with Duncan *post-hoc* test).

similar extent to that in *Col-0*, with slight sensitivity to Fe observed in the *pin2-1* mutant. *DR5:GFP* expression was further analyzed in roots treated with excess Fe plus cPTIO. Although cPTIO co-treatment relieved the Fe-mediated inhibition of root growth, it had no effect on *DR5:GFP* expression (Fig. S11c).

Recent studies (Reyt *et al.*, 2015; Onaga *et al.*, 2016) have suggested that Fe homeostasis interferes with ROS distribution in the primary root, and that this interaction may contribute to NO-mediated primary root shortening under Fe excess. Consistently, excess Fe significantly induced ROS in the root tip zone of both *Col-0* and *nox1* seedlings (Fig. S12); however, the ROS levels in *nox1* did not differ significantly from those in *Col-0*.

### NO contributes to excess Fe-mediated $K^+$ depletion and cell death in the root tip zone

Given that excess Fe markedly induced root tip  $K^+$  loss (cf Figs 2, 3), we asked whether endogenous NO levels in Fe-treated plants were related to  $K^+$  loss in root tips exposed to Fe stress. As shown in Fig. 7(a,b), the pretreatment of *Arabidopsis* roots with the NO scavenger cPTIO reduced the excess Fe-induced *Col-0* root tip  $K^+$  efflux. By contrast, SNP pretreatment significantly enhanced  $K^+$  efflux in the *Col-0* tip zone under both control and Fe treatment conditions (Figs 7a,b, S13a). Moreover, the *nox1* mutant exhibited more  $K^+$  efflux in the root tip zone relative to *Col-0*

under both control and Fe treatment conditions (Figs 7c,d, S13b, c).  $Gd^{3+}$  pretreatment reduced the Fe-induced root tip  $K^+$  efflux in the *nox1* mutant (Fig. 7e,f). Moreover,  $Gd^{3+}$  did not affect excess Fe-induced NO levels in the *Col-0* root tip (Fig. S14). Imaging using the APG-2 fluorescent dye revealed a lower  $K^+$  level in the root tip zone of the *nox1* mutant than in *Col-0* under Fe stress (Fig. 8).

Fe excess and NO accumulation have also been reported to trigger cell death (Bai *et al.*, 2012; Li *et al.*, 2012). In these studies, the rate of regrowth of Fe-treated roots was significantly different from that of the controls, although the root growth of both *Col-0* and *nox1* following treatment was largely recovered after 24 h of recovery culture. Moreover, the regrowth rate of *nox1* was lower than that in *Col-0* (Fig. S15a). We further stained roots with excess Fe using TB staining (Duan *et al.*, 2010). Compared with the control, exposure to excess Fe led to increased TB staining intensity at the root tip zone, and the TB staining intensity in *nox1* was significantly higher than that in *Col-0* (Fig. S15b). We also tested the effect of  $K^+$  deficiency under excess Fe on TB staining at the root tip zone.  $K^+$  deficiency significantly enhanced *Col-0* root tip zone TB staining under Fe toxicity (Fig. S6d).

*SNO1/SOS4* has been reported to be a critical factor of NO modulation of  $K^+$  levels in *Arabidopsis* roots and the activity is induced by NO (Xia *et al.*, 2014). Consistently, *SNO1/SOS4*

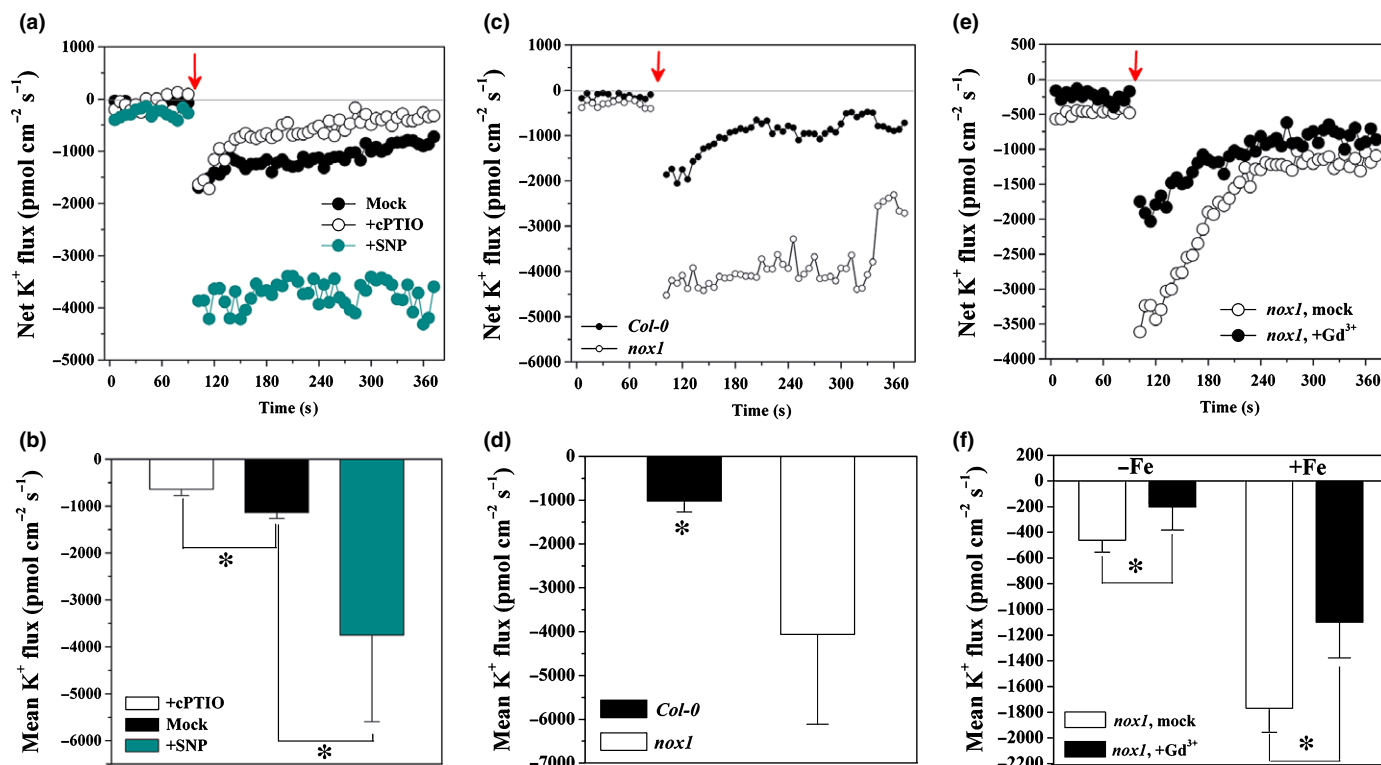


**Fig. 7** Effects of nitric oxide (NO) on excess iron (Fe)-mediated net plasma membrane  $K^+$  fluxes in the *Arabidopsis thaliana* root tip zone. (a) Effect of 2-(4-carboxyphenyl)-4,4,5,5-tetramethylimidazoline-1-oxyl-3-oxide (cPTIO) (100  $\mu$ M) and sodium nitroprusside (SNP) (15  $\mu$ M) pretreatment on net  $K^+$  fluxes from epidermal root cells in the *Col-0* root apical zone in response to 300  $\mu$ M Fe (indicated by the arrow). (b) Mean values of  $K^+$  fluxes from (a). Asterisk denotes statistical significance ( $n \geq 3$ , independent samples  $t$ -test,  $P < 0.05$ ). (c) Effects of excess Fe on net  $K^+$  fluxes at the root apical transition zone of *Col-0* and the *nox1* mutant. (d) Mean values of  $K^+$  fluxes from (c). Asterisk denotes statistical significance. (e) Effect of  $Gd^{3+}$  (50  $\mu$ M) pretreatment on net  $K^+$  fluxes from epidermal root cells in the *nox1* root apical zone in response to 300  $\mu$ M Fe. (f) Mean values of  $K^+$  fluxes from (e). Asterisks denote statistical significance ( $n \geq 3$ , independent samples  $t$ -test,  $P < 0.05$ ). Values shown are the means  $\pm$  SD.

activity was increased in SNP-treated *Col-0* seedlings compared with controls (Fig. 9a). In addition, an increase in *SNO1/SOS4* activity was observed in Fe-treated *Col-0* and *nox1* seedlings; however, the induction was more significant in *nox1* (Fig. 9a). Moreover, compared with *Col-0* controls, the *sno1/sos4* mutant exhibited aggravated root growth inhibition and significantly greater root tip zone  $K^+$  efflux in response to excess Fe (Fig. 9b–d). The elevated PLP content directly mediated by increased *SNO1/SOS4* activity has been reported to play a role in the regulation of  $K^+$  currents (Xia *et al.*, 2014). In this study, PLP pretreatment significantly enhanced the excess Fe-induced  $K^+$  efflux in the *Col-0* root tip zone, and application of  $Gd^{3+}$  reversed the PLP-induced  $K^+$  efflux under excess Fe (Fig. 9e,f). Seedlings grown under  $K^+$  addition plus cPTIO showed well-developed root growth compared with  $K^+$  addition alone (Fig. S16a). However, no significant alleviation by  $K^+$  addition was observed in *nox1* and *sno1/sos4* mutants under Fe stress, compared with *Col-0* (Fig. S16b), even when exogenous  $K^+$  was increased to 10 mM (data not shown).

### Ethylene negatively regulates excess Fe-induced NO accumulation

Ethylene has been suggested to alleviate Fe toxicity in some cases. The *AtACS7* gene has been reported to play a key role

in excess Fe-induced ethylene production (Li *et al.*, 2015a,b); herein, *AtACS7::GUS* activity, in which the GUS reporter gene is driven by the *AtACS7* promoter, was markedly increased in the root tip under excess Fe (Fig. 10a). Consistent with this, *EBS::GUS* expression (an ethylene reporter construct in which the GUS reporter gene is driven by a synthetic EIN3-responsive promoter) was also enhanced markedly in the root tip zone under Fe excess (Fig. S17). Supplementation with AVG, an inhibitor of ethylene biosynthesis, aggravated the inhibition of primary root growth under Fe excess (Fig. 10b). Meanwhile, *eto2-1*, a gain-of-function *ACS5* mutant allele of *ETO2*, which confers increased ethylene production (Wang *et al.*, 2004), displayed increased root growth tolerance compared with *Col-0* (Fig. 10c).

As ethylene and NO are both involved in the regulation of root growth under Fe excess, their roles need to be determined. NO-dependent fluorescence in root tips was significantly increased in the presence of the ethylene inhibitor AVG under Fe excess (Fig. 10d). This was further supported by the observation that Fe-induced NO generation in root tips was lower in *eto2-1* than in *Col-0* (Fig. 10e). Interestingly, application of the NO donor SNP increased *AtACS7::GUS* expression in the root tip under excess Fe, compared with the mock condition (Fig. S18). We further examined the role of ethylene in Fe-regulated  $K^+$  fluxes. In *Col-0* plants, AVG pretreatment significantly enhanced Fe-



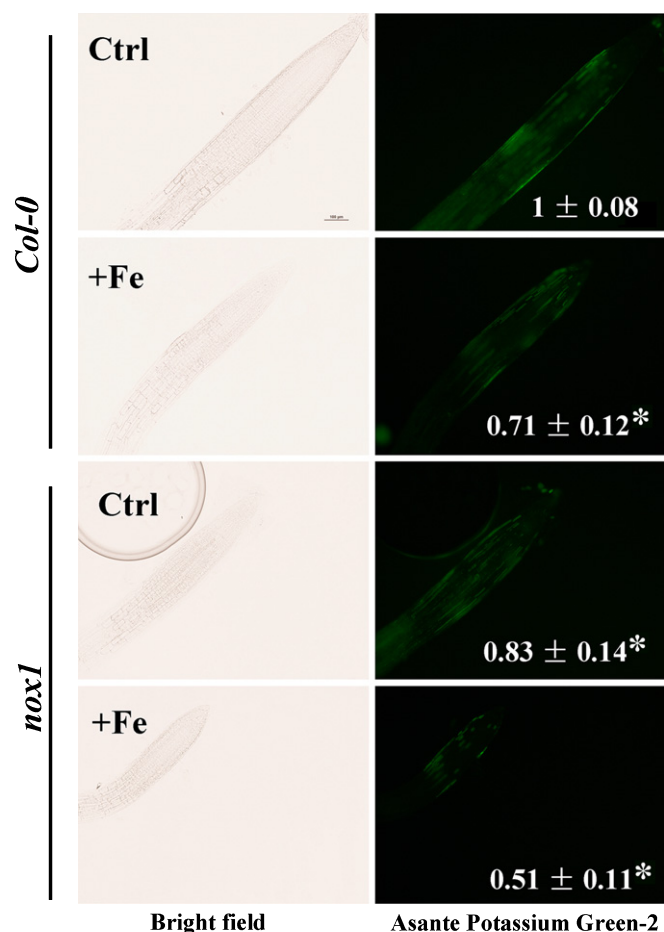


**Fig. 8** Effect of excess iron (Fe) on Asante Potassium Green-2 (APG-2) staining in the *Arabidopsis thaliana* Col-0 and *nox1* root tip zone. Five-day-old seedlings exposed to excess Fe for 3 d before staining with a K<sup>+</sup> indicator (APG-2). Bar, 100  $\mu$ m. The quantification of samples is shown in the images, and the fluorescence intensity of the Col-0 control root tip zone was set to 1. Asterisks denote statistical significance compared with Col-0 control (independent samples *t*-test,  $P < 0.05$ ). Values shown are the means  $\pm$  SD ( $n = 10$ –12).

induced K<sup>+</sup> efflux in the root tip zone compared with the mock condition (Fig. 10f,g).

## Discussion

Previous observations and our present results show that excess Fe supplied to *Arabidopsis* roots can regulate the distal organizer pattern in the root tip (Reyt *et al.*, 2015; Fig. 2a,b). Excess Fe-induced root growth inhibition requires that the root tip be in direct contact with external Fe, and the root tip zone is more sensitive than other root zones to Fe toxicity (Zhang *et al.*, 2011; Li *et al.*, 2015b; Fig. 1c). However, it has remained unclear what processes underpin the higher sensitivity of the root tip to Fe stress. In our study, we found that the higher Fe sensitivity was related, at least in part, to compromised K<sup>+</sup> retention in the root apical zone. Further examination revealed that the sensitivity of the root tip zone, the impairment of K<sup>+</sup> homeostasis in that zone and cell death under Fe toxicity were associated with Fe-induced

NO accumulation. To assist in the interpretation of a complex dataset that highlights the importance of NO accumulation and K<sup>+</sup> homeostasis responses to excess Fe, we provide a model to explain the growth inhibition of root apical tissues at the molecular and physiological level (Fig. 11).

The maintenance of sufficient K<sup>+</sup> levels enhances plant tolerance to various environmental stresses (Kronzucker *et al.*, 2008; Britto & Kronzucker, 2009; Szczerba *et al.*, 2009; Coskun *et al.*, 2010, 2013a; Li *et al.*, 2014). A strong positive correlation between the ability to retain K<sup>+</sup> and Fe excess tolerance has been reported previously in rice (Onaga *et al.*, 2016), *Epilobium hirsutum* (Wheeler *et al.*, 1985) and *Arabidopsis* (Li *et al.*, 2016a). Although excess Fe has been reported previously to inhibit root growth by the negative regulation of K<sup>+</sup> homeostasis (Li *et al.*, 2001, 2015b; Çelik *et al.*, 2010), how Fe excess impacts root K<sup>+</sup> homeostasis has remained rather poorly understood. In our study, we found that Fe excess-induced K<sup>+</sup> loss was especially pronounced in the root tip zone. Root apical zones showed greater K<sup>+</sup> efflux and retained less K<sup>+</sup> when exposed to Fe excess (Figs 2, 3), and K<sup>+</sup> deficiency in root apical zones could aggravate excess Fe-inhibited root growth inhibition (Figs S3, S6a). Cells that are not completely differentiated, especially those in the root meristem, are characterized by a small vacuole, low volume, low water content and low fresh weight (Luxova, 1988). Shabala *et al.* (2006) suggested that higher net K<sup>+</sup> efflux implies lower cytosolic K<sup>+</sup>, which could alter cell elongation processes. K<sup>+</sup> efflux across the root plasma membrane has been reported to be mainly mediated by GORK and NSCCs (Coskun *et al.*, 2010; Demidchik, 2014; Shabala *et al.*, 2016). Copper ascorbate-induced K<sup>+</sup> loss from *Arabidopsis* roots is mediated by K<sup>+</sup>-selective channels (K<sup>+</sup> loss was blocked by TEA and reduced in the *gork1* mutant) (Demidchik *et al.*, 2010). However, both TEA pretreatment and GORK1 mutation had no significant effect on the root tip K<sup>+</sup> efflux under excess Fe (Fig. 4). A persistent lack of certainty around which molecular candidates code for NSCCs, and the lack of clear phenotypes in loss-of-function mutants, present a significant challenge in studies of NSCCs and in attempts to relate their function mechanistically to a number of physiological phenomena (Kronzucker & Britto, 2011; Pottosin & Dobrovinskaya, 2014). Pharmacological NSCC blockers, such as Gd<sup>3+</sup>, which tend to display broader spectrum inhibition (Kronzucker & Britto, 2011), are, however, widely used in studies on NSCCs; for example Zepeda-Jazo *et al.* (2011) suggested that copper ascorbate-induced K<sup>+</sup> efflux from pea roots is mediated by NSCCs by using evidence derived from Gd<sup>3+</sup>. Here, a large contribution of NSCCs is suggested by the fact that Gd<sup>3+</sup> caused a *c.* 60% inhibition of excess Fe-induced K<sup>+</sup> efflux (Fig. 4a,b), and application of Gd<sup>3+</sup> mildly alleviated the decrease in the rate of root growth under Fe toxicity (Fig. S5a). Furthermore, our present and previous data show that suppression of root growth under excess Fe can be significantly alleviated by K<sup>+</sup> addition (Li *et al.*, 2016a; Fig. S6a), and K<sup>+</sup> addition can lead to higher tissue K levels (Fig. S6c), supporting the importance of the role of K<sup>+</sup> retention in tolerance to excess Fe.

In contrast with the study of the role of NO in the response to Fe limitation, the possible roles of NO in the regulation of root

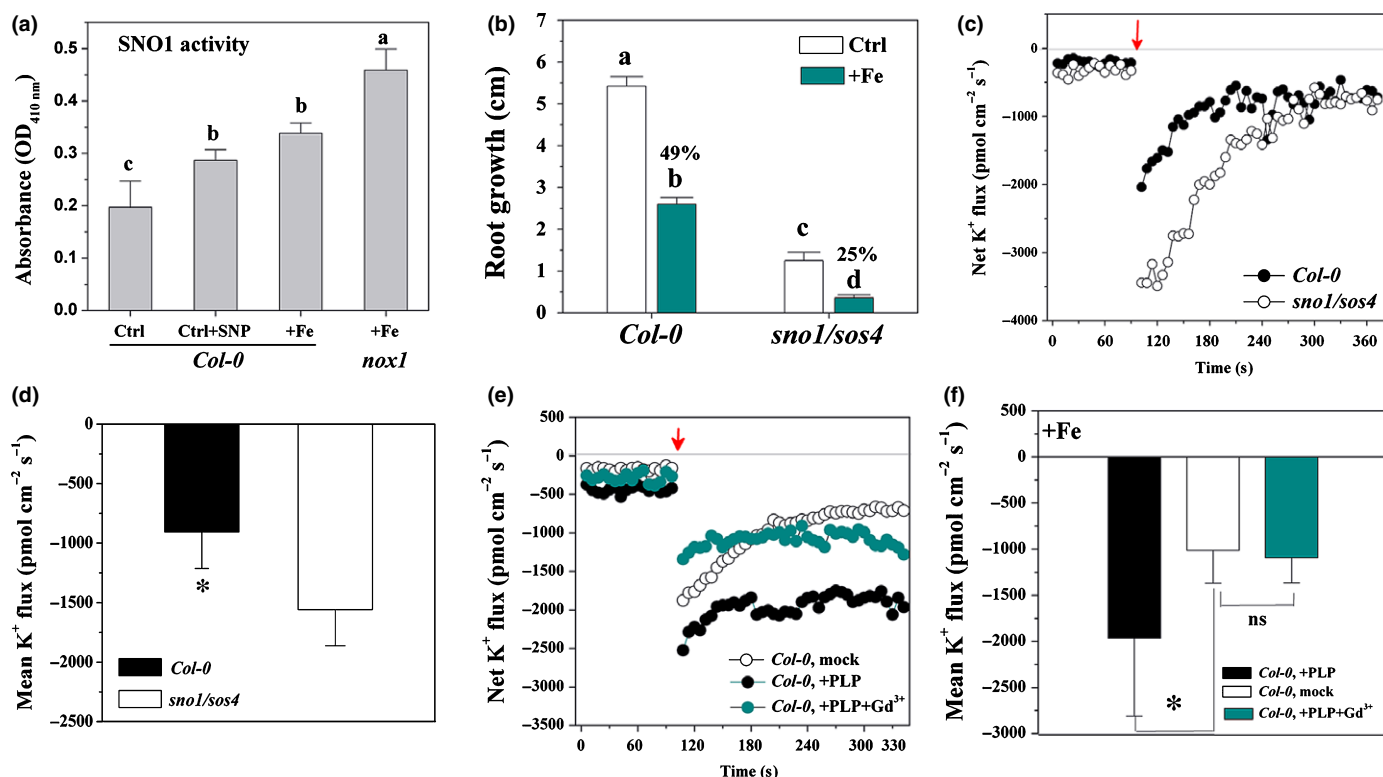


**Fig. 9** Effects of SNO1 (sensitive to nitric oxide 1)/SOS4 (salt overly sensitive 4) on iron (Fe)-mediated root growth and net plasma membrane K<sup>+</sup> fluxes in the *Arabidopsis thaliana* root tip zone. (a) Enzyme activity of SNO1/SOS4 in *Col-0* and *nox1* roots in response to sodium nitroprusside (SNP) (15  $\mu$ M) and excess Fe (300  $\mu$ M). Seven-day-old seedlings exposed to excess Fe for 3 d. Different letters represent means that are statistically significantly different at the 0.05 level (one-way ANOVA with Duncan *post-hoc* test). (b) Effect of excess Fe on primary root growth in *Col-0* and the *sno1/sos4* mutant. Five-day-old seedlings exposed to excess Fe for 5 d. Different letters represent means that are statistically significantly different at the 0.05 level (one-way ANOVA with Duncan *post-hoc* test) ( $n = 10$ ). (c) Effects of excess Fe (indicated by the arrow) on net K<sup>+</sup> fluxes at the root apical transition zone of *Col-0* and *sno1/sos4* mutant seedlings. (d) Mean values of K<sup>+</sup> fluxes from (c). Asterisk denotes statistical significance ( $n \geq 3$ , independent samples *t*-test,  $P < 0.05$ ). (e) Effect of pyridoxal-5'-phosphate (PLP) (100  $\mu$ M) and PLP plus Gd<sup>3+</sup> (50  $\mu$ M) pretreatment on net K<sup>+</sup> fluxes from epidermal root cells in the *Col-0* root apical zone in response to 300  $\mu$ M Fe (indicated by the arrow). (f) Mean values of K<sup>+</sup> fluxes under excess Fe from (e). Asterisk denotes statistical significance ( $n \geq 4$ , independent samples *t*-test,  $P < 0.05$ ; ns, nonsignificant). Values shown are the means  $\pm$  SD.

growth under Fe surplus have not been investigated. In this study, we have demonstrated that root growth effects under Fe excess are mediated, at least in part, by NO accumulation (Figs 5, 6). To cope with Fe deficiency, plants must ensure effective Fe acquisition from the rhizosphere. Fe deficiency-induced NO can trigger the expression of the *FIT* gene, which regulates the expression of *FRO2* and *IRT*, to increase the uptake of Fe (Chen *et al.*, 2010). By contrast, under excess Fe conditions, restriction of excessive Fe absorption can prevent more serious Fe toxicity (Becker & Asch, 2005), and the expression of the *IRT1* gene is significantly inhibited at high Fe concentrations (Giehl *et al.*, 2012). The function of NO in the promotion of Fe uptake is useful in the acclimation to Fe deficiency, but does not seem to be conducive to improving the responses to excess Fe conditions. It is, however, not known whether NO may directly modulate root Fe influx and/or efflux under excess Fe, and more research is warranted to examine this. Other metals, such as Cu and Al, have also been shown to produce oxidative stress and to inhibit root growth (Xiong *et al.*, 2010), but, in contrast with excess Fe stress, NO plays a positive role in Cu and Al toxicity tolerance in relation to root growth (Tian *et al.*, 2007; Peto *et al.*, 2013; Liu *et al.*,

2016; Fig. S10), although NO plays a negative role in Al tolerance in some plants, such as rice bean (Zhou *et al.*, 2012). Thus, it can be hypothesized that, depending on the biological context, NO exerts opposing effects on root growth. L-NAME (a NOS inhibitor) has been reported to reduce salt-induced NO production in *Arabidopsis* (Liu *et al.*, 2015), and L-NAME can reduce the inhibitory effect of salt treatment on root growth (Liu *et al.*, 2015; Fig. S7b). Chen *et al.* (2010) have demonstrated that NOS and the *NOA1* gene are involved in Fe deficiency-regulated NO generation in the *Arabidopsis* root tip zone, and Fe deficiency-induced NO accumulation and gene expression are significantly suppressed by the NOS-inhibitor L-NAME and by the *NOA1* mutation. By contrast, Touraine *et al.* (2012) clearly showed that treatment with L-NAME or L-NMMA and the mutation in *NOA1* did not affect Fe excess-dependent NO production in *Arabidopsis*. Our present data show that L-NAME or L-NMME and the mutation in *NOA1* have no significant effect on excess Fe-inhibited root growth (Fig. S7a,c), supporting the results of Touraine *et al.* (2012). All the results to date suggest that the regulatory mechanisms underpinning NO accumulation in *Arabidopsis* are fundamentally different in response to Fe

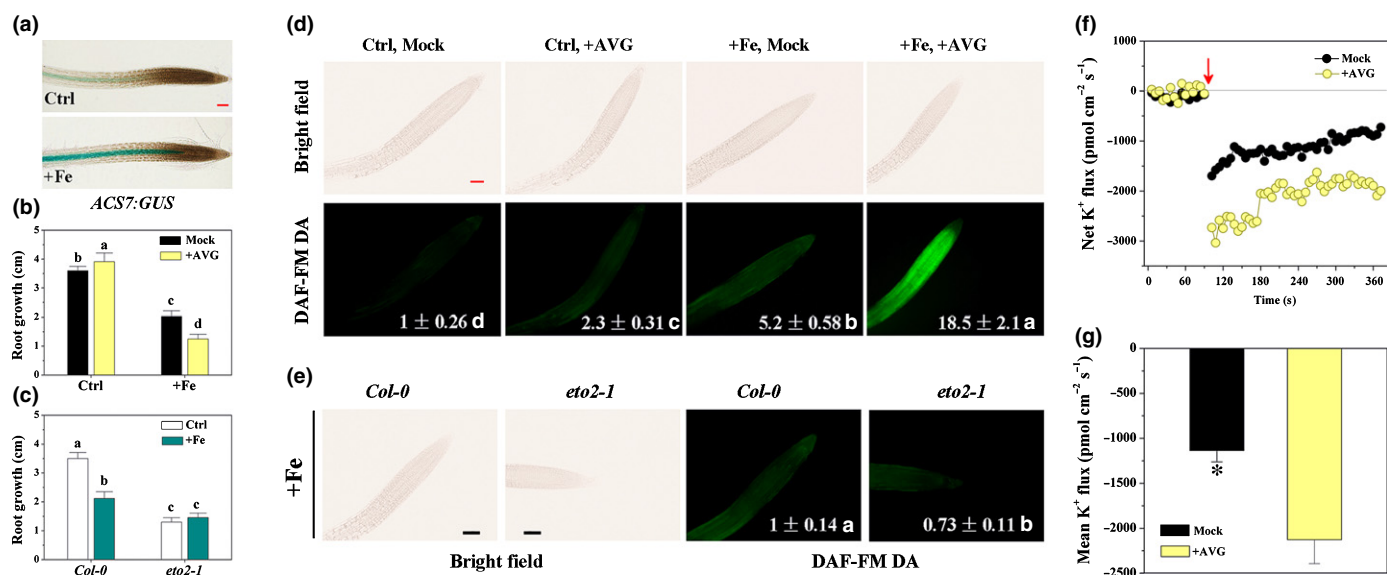


**Fig. 10** Effects of ethylene on iron (Fe)-mediated root growth, nitric oxide (NO) production and net plasma membrane K<sup>+</sup> fluxes in the *Arabidopsis thaliana* root tip zone. (a) Activity of *AtACS7:GUS* (ACS, 1-aminocyclopropane-1-carboxylic acid synthase) in *Arabidopsis* root tissue. Five-day-old seedlings exposed to excess Fe for 2 d. One representative sample from each treatment (seven plants) is shown. (b) Effect of the ethylene inhibitor aminoethoxyvinylglycine (AVG) (0.75 μM) on the primary root growth of *Col-0* seedlings grown in control and Fe treatment media. Five-day-old seedlings exposed to excess Fe for 3 d. (c) Effect of excess Fe on primary root growth in *Col-0* seedlings and the ethylene-overproducing mutant *eto2-1*. (d) Effect of the ethylene inhibitor AVG (0.75 μM) on NO production in the root tip zone. Five-day-old seedlings exposed to excess Fe for 2 d. One representative sample from each treatment ( $n = 14-15$ ) is shown, and the fluorescence intensity of control mock root tip zone was set to 1. DAF-FM DA, 3-amino,4-aminomethyl-2',7'-difluorescein, diacetate. (e) Effects of excess Fe on the production of NO in roots of *Arabidopsis Col-0* and *eto2-1* plants. Five-day-old seedlings exposed to excess Fe for 2 d. One representative sample from each treatment ( $n = 11-12$ ) is shown, and the fluorescence intensity of the *Col-0* root tip zone was set to 1. (f) Effect of AVG (0.75 μM) pretreatment on net K<sup>+</sup> fluxes from epidermal root cells in the root apical zone in response to 300 μM Fe (indicated by the arrow). (g) Mean values of K<sup>+</sup> fluxes from (f). Asterisk denotes statistical significance (independent samples *t*-test,  $P < 0.05$ ). Values shown are the means  $\pm$  SD ( $n \geq 3$ ). Different letters represent means statistically different at the 0.05 level (one-way ANOVA with Duncan *post-hoc* test). Ctrl, control (50 μM Fe); +Fe, excess Fe (300 μM Fe). Bars, 100 μm.

deficiency as opposed to Fe excess. NO production from different sources may result in divergent effects (Xiong *et al.*, 2010), even in response to the same stress. For example, nitrate reductase (NR)-mediated, rather than NOS- and other source-mediated, NO bursts are involved in the protection against Al toxicity in roots of wheat (Sun *et al.*, 2014). At least seven possible pathways of NO biosynthesis have been described in plants (Gupta *et al.*, 2011). However, to date, the mechanisms underlying the induction of NO biosynthesis under excess Fe in plants is still largely unknown. Further studies on the precise origin of excess Fe-induced NO in plant tissues are warranted.

The question then arises as to how Fe-induced NO accumulation leads to impaired resistance to Fe excess. It has been suggested that NO can suppress root growth by reducing auxin in root tips under salt and Cd stress (Liu *et al.*, 2015; Yuan & Huang, 2016). However, unlike in salt or Cd stress, the *DR5*-indicative auxin level in the root tip was not reduced under excess Fe, although an NO burst and inhibition of root growth were observed over the same treatment time. All these observations further illustrate the complexity and variation in NO-mediated root development when responding to the different environmental stresses. Alternatively, increased ROS levels are also involved in excess Fe-inhibited primary root length (Reyt *et al.*, 2015) and are the stimulus to activate NSCCs, resulting in K<sup>+</sup> loss from the cell (Pottosin & Dobrovinskaya, 2014; Shabala *et al.*, 2016). In

agreement with the observations of Reyt *et al.* (2015), excess Fe indeed increased the ROS level in root tips of both *Col-0* and *nox1* seedlings (Fig. S12); however, the elevated ROS levels in *nox1* did not significantly differ from those in *Col-0* in our study, suggesting that the ROS increase caused by Fe excess is not the main reason for impaired Fe resistance in *nox1*. Meanwhile, it is important to recall that NO can increase the abundance of ferritin proteins which store Fe to avoid oxidative stress (Arnaud *et al.*, 2006; Briat *et al.*, 2010). However, Reyt *et al.* (2015) has clearly demonstrated, using genetic evidence, that ferritin is not involved in the modulation of primary root growth under excess Fe. The work described in this article further shows that Fe-induced NO accumulation is involved in Fe-dependent root tip zone K<sup>+</sup> homeostasis based on pharmacological and genetic evidence. According to the literature, the effects of NO on root K<sup>+</sup> homeostasis can vary greatly between conditions and plant species. Chen *et al.* (2013) showed that SNP increases K<sup>+</sup> content under exposure to salt in *Kandelia obovata*. However, Xia *et al.* (2014) found that SNP can mediate root K<sup>+</sup> homeostasis by the negative regulation of root K<sup>+</sup> uptake via suppression of the AKT1 gene in *Arabidopsis*. Cd induces NO, but has no effect on *Arabidopsis* root K<sup>+</sup> status (Besson-Bard *et al.*, 2009). These diverse results on the relationships between NO and K<sup>+</sup> homeostasis might be attributed to the impacts of external stimuli on NO content and different sources of NO production in plants.



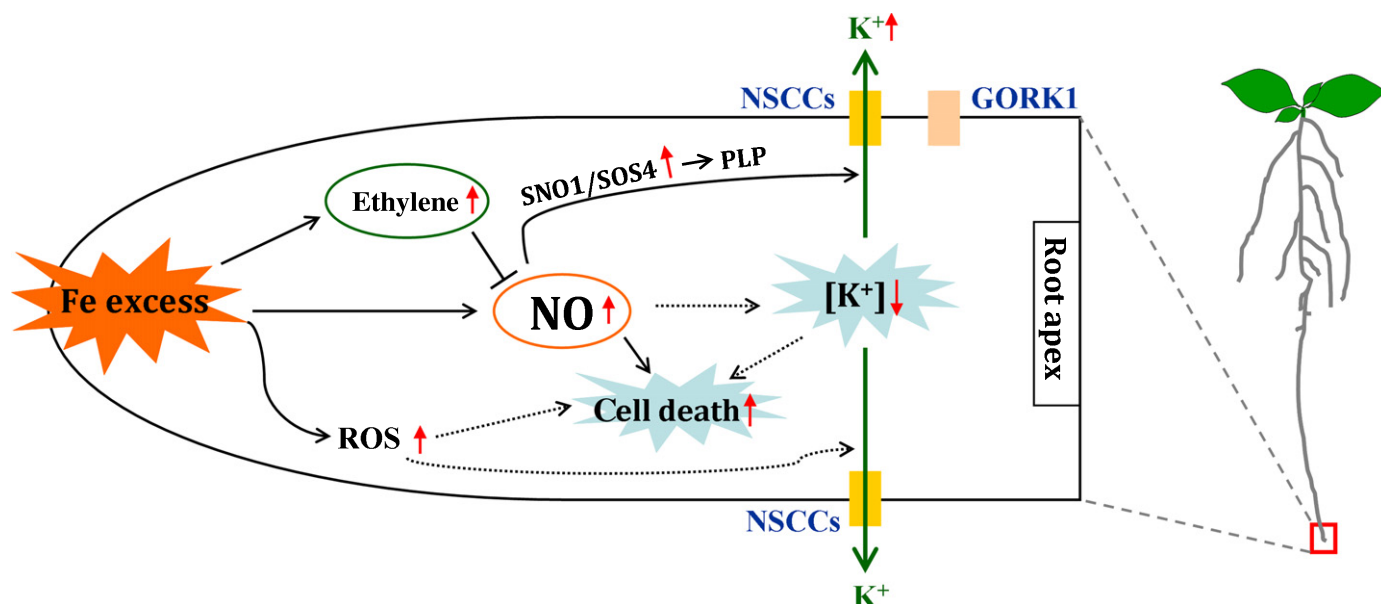


**Fig. 11** A proposed model for nitric oxide (NO)-mediated *Arabidopsis thaliana* primary root tip zone growth under iron (Fe) excess. NO levels in root tips are increased significantly above levels elsewhere in the root and are involved in the arrest of primary root tip zone growth under excess Fe. NO-mediated inhibition of root growth is, at least in part, related to NO-induced  $K^+$  loss via nonselective cation channels (NSCCs), and increased *SNO1* (sensitive to nitric oxide 1)/*SOS4* (salt overly sensitive 4) activity-mediated pyridoxal-5'-phosphate (PLP) is further implicated in this process. NO also mediates  $K^+$  homeostasis by the negative regulation of  $K^+$  uptake. The significant  $K^+$  loss can result in the loss of cell turgor (and hence arrest root growth) and either programmed cell death (PCD) or necrosis in the root apex. Meanwhile, excess Fe also reduces cell viability, associated with reactive oxygen species (ROS) accumulation and NO-induced hormone imbalance and protein S-nitrosylation. ROS has also been reported to activate NSCCs, resulting in  $K^+$  loss from the cell. Furthermore, Fe-induced ethylene can partially antagonize the reduction in excess Fe-mediated primary root growth by the control of NO levels. GORK1, guard cell outward-rectifying  $K^+$  channel 1.

Although the mechanism by which endogenous NO regulates root tip  $K^+$  efflux under excess Fe remains to be defined, one hypothesis is that NO might influence ion channels in roots.  $Gd^{3+}$  pretreatment significantly decreased root tip  $K^+$  efflux in the *nox1* mutant under both control and Fe treatment (Fig. 7e, f). Recently, it has been reported that enhanced NO accumulation could indirectly, via *SNO1/SOS4*, result in a reduction in  $K^+$  uptake in the root (Xia *et al.*, 2014). Here, we have provided evidence that an increase in *SNO1/SOS4* activity was observed in the excess Fe-treated *Col-0* and *nox1* seedlings, and that the induction was more significant in *nox1* (Fig. 9a). The *SNO1/SOS4* gene is also involved in root growth and the regulation of root tip zone  $K^+$  fluxes under Fe toxicity (Fig. 9b–d). It is not known at this time how the *SNO1/SOS4* gene engages to modulate root tip  $K^+$  efflux. Xia *et al.* (2014) have demonstrated that increased *SNO1/SOS4* activity can trigger PLP accumulation and that PLP plays a critical role in the regulation of *Arabidopsis* root  $K^+$  content. PLP can stimulate root tip  $K^+$  efflux under excess Fe. In our study, PLP pretreatment enhanced excess Fe-induced  $K^+$  efflux in the *Col-0* root tip zone, and application of  $Gd^{3+}$  reversed the PLP-induced  $K^+$  efflux under excess Fe (Fig. 9e,f). More detailed research is warranted to examine this in the future. Interestingly, there was no significant alleviation of Fe-inhibited root growth by  $K^+$  addition in *nox1* and *sno1/sos4* mutants, suggesting that NO might negatively regulate additional  $K^+$  alleviation of Fe excess. One hypothesis is that the overaccumulation of NO could reduce  $K^+$

uptake (Xia *et al.*, 2014), and this might restrict the tissue  $K^+$  concentration under  $K^+$  addition.

Excess Fe and NO accumulation have been reported to trigger cell death (Xu *et al.*, 2010; Bai *et al.*, 2012), although the mechanism for this is not understood. Excess Fe induced ROS accumulation (Reyt *et al.*, 2015; Fig. S12), which could trigger oxidative damage and cell death (Lin *et al.*, 2012). In this study, the *nox1* mutant showed more severe root tip cell mortality, but similar ROS accumulation, to *Col-0* under Fe toxicity (Fig. S12), suggesting that NO may also be involved in Fe-induced cell death. Previous reports have suggested that NO-induced cell death is related to NO-mediated hormone imbalance and protein S-nitrosylation (Xu *et al.*, 2010; Bai *et al.*, 2012; Lin *et al.*, 2012). In addition,  $K^+$  loss can stimulate cell death in animals and in *Arabidopsis* (Yu, 2003; Demidchik *et al.*, 2010). Consistent with this,  $K^+$  deficiency significantly enhanced *Col-0* root tip zone TB staining-indicated cell death under Fe toxicity in our study (Fig. S6d). More research is warranted to examine this.

Ethylene is regarded as a stress hormone and can be induced by a variety of stresses to protect growth, such as under salt stress (Jiang *et al.*, 2013), but ethylene accumulation in non-stressed environments can inhibit root growth (Fig. 10c), partly associated with induced hormonal imbalance (e.g. auxin, jasmonates and abscisic acid (ABA)) (Adams & Turner, 2010; Strader *et al.*, 2010; Ma *et al.*, 2014). Ethylene has been shown to play a role in the tolerance of primary root growth to excess Fe (Peng &



Yamauchi, 1993; Li *et al.*, 2015b; Fig. 10), although specific mechanisms for this have remained unclear. Here, we suggest that one possible mechanism of ethylene-induced tolerance of primary root growth in *Col-0* occurs partly through NO mediation. The findings are also consistent with previous reports showing that ethylene regulates NO levels in plants (Song *et al.*, 2011; Liu *et al.*, 2017). Interestingly, treatment with the NO donor SNP stimulates *ACS7* gene expression in the root under Fe excess, suggesting that ethylene production can respond to NO levels under Fe excess. Supportive of this are the findings by Gniazdowska *et al.* (2007) and Liu *et al.* (2017), showing that SNP upregulates the activities of ethylene biosynthesis enzymes.

In conclusion, NO levels in root tips are increased significantly above levels elsewhere in the root and are involved in the arrest of primary root tip zone growth under excess Fe. Fe-inhibited root growth is, at least in part, related to NO-induced K<sup>+</sup> loss, possibly via NSCCs. Meanwhile, excess Fe also affects cell viability, probably via ROS accumulation, NO-induced hormone imbalance and protein S-nitrosylation, all of which affect root growth. These modulations in hormone and K<sup>+</sup> homeostasis might regulate the growth rate to reduce the interceptive surface of the root system to excess Fe. Meanwhile, ethylene can partially antagonize the reduction in excess Fe-mediated primary root growth by the control of NO levels. These compensatory effects of ethylene may prevent the excessive decline in root growth and maintain the absorption of other nutrients (Heil & Baldwin, 2002). In addition, the root hair zone is more tolerant to Fe excess and can sequester more Fe in the vacuole, cell wall and by components to avoid the deposition of excessive Fe in susceptible tissues (such as the root tip zone). Further research into the interplay of ion homeostasis and NO will enable a fuller understanding of how plants respond to Fe toxicity by the regulation of hormonal and ion signaling.

## Acknowledgements

We thank Drs Caifu Jiang (China Agricultural University), Tom Guilfoyle (University of Missouri), Ben Scheres (Utrecht University) and Ningning Wang (Nankai University) for providing the seeds of *eto2-1*, *DR5:GUS*, *DR5:GFP* and *ACS7:GUS* lines, respectively, Dr GuangQin Guo (Lanzhou University), Dr J. Alonso (North Carolina State University) and Dr Yanhua Su (Institute of Soil Science) for providing seeds of *DR5:GUS* in *wei7-2*, *EBS:GUS* reporter lines and *gork1* mutant, respectively, and the Arabidopsis Biological Resource Center of Ohio State University for mutant seeds. This work was supported by the National Natural Science Foundation of China (31430095), the National Key R&D Program of China (2017YFD0200103), the National Natural Science Foundation of China (31501821), the Chinese Academy of Sciences Innovation Program (CAS ISSASIP1604) and the University of Melbourne.

## Author contributions

L.Z. and G.L. executed the experiments, interpreted the data, generated the figures and were the major writers of the article.

W.S. was involved in the design of the experiments, analysis and interpretation of the data and, together with L.Z. and G.L., was the major writer of the article. H.J.K. assisted in discussion and the writing of the article. M.W., D.D. and L.S. assisted in discussion. L.Z. and G.L. contributed equally to this work.

## References

- Adams E, Turner J. 2010. COI1, a jasmonate receptor, is involved in ethylene-induced inhibition of *Arabidopsis* root growth in the light. *Journal of Experimental Botany* 61: 4373–4386.
- Alemayehu A, Zelinová V, Bočová B, Huttová J, Mistrík I, Tamás L. 2015. Enhanced nitric oxide generation in root transition zone during the early stage of cadmium stress is required for maintaining root growth in barley. *Plant and Soil* 390: 213–222.
- Arnaud N, Murgia I, Boucherez J, Briat JF, Cellier F, Gaymard F. 2006. An iron-induced nitric oxide burst precedes ubiquitin-dependent protein degradation for *Arabidopsis AtFer1* ferritin gene expression. *Journal of Biological Chemistry* 281: 23579–23588.
- Bai S, Li M, Yao T, Wang H, Zhang Y, Xiao L, Wang J, Zhang Z, Hu Y, Liu W *et al.* 2012. Nitric oxide restrains root growth by DNA damage induced cell cycle arrest in *Arabidopsis thaliana*. *Nitric Oxide* 26: 54–60.
- Becker M, Asch F. 2005. Iron toxicity in rice—conditions and management concepts. *Journal of Plant Nutrition and Soil Science* 168: 558–573.
- Besson-Bard A, Gravot A, Richaud P, Auroy P, Duc C, Gaymard F, Taconnat L, Renou JP, Pugin A, Wendehenne D. 2009. Nitric oxide contributes to cadmium toxicity in *Arabidopsis* by promoting cadmium accumulation in roots and by up-regulating genes related to iron uptake. *Plant Physiology* 149: 1302–1315.
- Briat JF, Ravet K, Arnaud N, Duc C, Boucherez J, Touraine B, Cellier F, Gaymard F. 2010. New insights into ferritin synthesis and function highlight a link between iron homeostasis and oxidative stress in plants. *Annals of Botany* 10: 811–822.
- Britto DT, Kronzucker HJ. 2009. Ussing's conundrum and the search for transport mechanisms in plants. *New Phytologist* 183: 243–246.
- Çelik H, Asik BB, Gürel S, Katkat AV. 2010. Potassium as an intensifying factor for iron chlorosis. *International Journal of Agriculture and Biology* 12: 359–364.
- Chen J, Xiong DY, Wang WH, Hu WJ, Simon M, Xiao Q, Chen J, Liu TW, Liu X, Zheng HL. 2013. Nitric oxide mediates root K<sup>+</sup>/Na<sup>+</sup> balance in a mangrove plant, *Kandelia obovata*, by enhancing the expression of AKT1-type K<sup>+</sup> channel and Na<sup>+</sup>/H<sup>+</sup> antiporter under high salinity. *PLoS ONE* 8: e71543.
- Chen WW, Yang JL, Qin C, Jin CW, Mo JH, Ye T, Zheng SJ. 2010. Nitric oxide acts downstream of auxin to trigger root ferric-chelate reductase activity in response to iron deficiency in *Arabidopsis*. *Plant Physiology* 154: 810–819.
- Connolly EL, Guerinot ML. 2002. Iron stress in plants. *Genome Biology* 3: 1–6.
- Coskun D, Britto DT, Jean YK, Kabir I, Tolay I, Torun AA, Kronzucker HJ. 2013a. K<sup>+</sup> efflux and retention in response to NaCl stress do not predict salt tolerance in contrasting genotypes of rice (*Oryza sativa* L.). *PLoS ONE* 8: e57767.
- Coskun D, Britto DT, Kronzucker HJ. 2010. Regulation and mechanism of potassium release from barley roots: an *in planta* <sup>42</sup>K<sup>+</sup> analysis. *New Phytologist* 188: 1028–1038.
- Coskun D, Britto DT, Li MY, Oh S, Kronzucker HJ. 2013b. Capacity and plasticity of potassium channels and high-affinity transporters in roots of barley and *Arabidopsis*. *Plant Physiology* 162: 496–511.
- Crawford NM, Guo FQ. 2005. New insights into nitric oxide metabolism and regulatory functions. *Trends in Plant Science* 10: 195–200.
- Demidchik V. 2014. Mechanisms and physiological roles of K<sup>+</sup> efflux from root cells. *Journal of Plant Physiology* 171: 696–707.
- Demidchik V, Cuin TA, Svistunenko D, Smith SJ, Miller AJ, Shabala S, Sokoluk A, Yurin V. 2010. *Arabidopsis* root K<sup>+</sup> efflux conductance activated by hydroxyl radicals: single-channel properties, genetic basis and involvement in stress-induced cell death. *Journal of Cell Science* 123: 1468–1479.

- Demidchik V, Maathuis FJM. 2007. Physiological roles of nonselective cation channels in plants: from salt stress to signalling and development. *New Phytologist* 175: 387–404.
- Demidchik V, Shabala SN, Coutts KB, Tester MA, Davies JM. 2003. Free oxygen radicals regulate plasma membrane  $\text{Ca}^{2+}$ - and  $\text{K}^{+}$ -permeable channels in plant root cells. *Journal of Cell Science* 116: 81–88.
- Duan YF, Zhang WS, Li B, Wang YN, Li KX, Sodmergen Han CY, Zhang YZ, Li X. 2010. An endoplasmic reticulum response pathway mediates programmed cell death of root tip induced by water stress in *Arabidopsis*. *New Phytologist* 186: 681–695.
- Giehl RF, Lima JE, von Wiren N. 2012. Localized iron supply triggers lateral root elongation in *Arabidopsis* by altering the AUX1-mediated auxin distribution. *Plant Cell* 24: 33–49.
- Gniazdowska A, Dobrzynska U, Babarczyk T, Bogatek R. 2007. Breaking the apple embryo dormancy by nitric oxide involves the stimulation of ethylene production. *Planta* 225: 1051–1057.
- Graziano M, Lamattina L. 2007. Nitric oxide accumulation is required for molecular and physiological responses to iron deficiency in tomato roots. *Plant Journal* 52: 949–960.
- Gupta KJ, Fernie AR, Kaiser WM, van Dongen JT. 2011. On the origins of nitric oxide. *Trends in Plant Science* 16: 1360–1385.
- Heil M, Baldwin IT. 2002. Fitness costs of induced resistance: emerging experimental support for a slippery concept. *Trends in Plant Science* 7: 61–67.
- Jiang CF, Belfield EJ, Cao Y, Smith YAJ, Harberd NP. 2013. An *Arabidopsis* soil-salinity-tolerance mutation confers ethylene-mediated enhancement of sodium/potassium homeostasis. *Plant Cell* 25: 3535–3552.
- Kronzucker HJ, Britto DT. 2011. Sodium transport in plants: a critical review. *New Phytologist* 189: 54–81.
- Kronzucker HJ, Szczerba MW, Schulze LM, Britto DT. 2008. Non-reciprocal interactions between  $\text{K}^{+}$  and  $\text{Na}^{+}$  ions in barley (*Hordeum vulgare* L.). *Journal of Experimental Botany* 59: 2793–2801.
- Li BH, Li GJ, Kronzucker HJ, Baluska F, Shi W. 2014. Ammonium stress in *Arabidopsis*: signaling, genetic loci, and physiological targets. *Trends in Plant Science* 19: 107–114.
- Li GJ, Kronzucker HJ, Shi WM. 2016a. Root developmental adaptation to Fe toxicity: mechanisms and management. *Plant Signaling & Behavior* 11: e117722.
- Li GJ, Kronzucker HJ, Shi WM. 2016b. The response of the root apex in plant adaptation to iron heterogeneity in soil. *Frontiers in Plant Science* 7: 344.
- Li GJ, Li BH, Dong GQ, Feng XY, Kronzucker HJ, Shi WM. 2013. Ammonium-induced shoot ethylene production is associated with the inhibition of lateral root formation in *Arabidopsis*. *Journal of Experimental Botany* 64: 1413–1425.
- Li GJ, Song HY, Li BH, Kronzucker HJ, Shi WM. 2015a. Auxin resistant1 and PIN-FORMED2 protect lateral root formation in *Arabidopsis* under iron stress. *Plant Physiology* 169: 2608–2623.
- Li GJ, Xu WF, Kronzucker HJ, Shi WM. 2015b. Ethylene is critical to the maintenance of primary root growth and Fe homeostasis under Fe stress in *Arabidopsis*. *Journal of Experimental Botany* 66: 2041–2054.
- Li H, Yang X, Luo AC. 2001. Ameliorating effect of potassium on iron toxicity in hybrid rice. *Journal of Plant Nutrition* 24: 1849–1860.
- Li Q, Li BH, Kronzucker HJ, Shi WM. 2010. Root growth inhibition by  $\text{NH}_4^{+}$  in *Arabidopsis* is mediated by the root tip and is linked to  $\text{NH}_4^{+}$  efflux and GMPase activity. *Plant, Cell & Environment* 33: 1529–1542.
- Li XN, Ma HZ, Jia PX, Wang J, Jia LY, Zhang TG, Yang YL, Chen HJ, Wei X. 2012. Responses of seedling growth and antioxidant activity to excess iron and copper in *Triticum aestivum* L. *Ecotoxicology and Environmental Safety* 86: 47–53.
- Lin AH, Wang YQ, Tang JY, Xue P, Li CL, Liu LC, Hu B, Yang FQ, Loake GJ, Chu CC. 2012. Nitric oxide and protein S-nitrosylation are integral to hydrogen peroxide-induced leaf cell death in rice. *Plant Physiology* 158: 451–464.
- Liu ML, Liu XX, He XL, Liu LJ, Wu H, Tang CX, Zhang YS, Jin CW. 2017. Ethylene and nitric oxide interact to regulate the magnesium deficiency-induced root hair development in *Arabidopsis*. *New Phytologist* 213: 1242–1256.
- Liu SL, Yang RJ, Pan YZ, Ren B, Chen QB, Li X, Xiong X, Tao JJ, Cheng QS, Ma MD. 2016. Beneficial behavior of nitric oxide in copper-treated medicinal plants. *Journal of Hazardous Materials* 314: 140–154.
- Liu W, Li RJ, Han TT, Cai W, Fu ZW, Lu YT. 2015. Salt stress reduces root meristem size by nitric oxide mediated modulation of auxin accumulation and signaling in *Arabidopsis*. *Plant Physiology* 168: 343–356.
- Ludewig U, Wilken S, Wu B, Jost W, Obrdlik P, El Bakkoury M, Marini AM, Andre B, Hamacher T, Boles E *et al.* 2003. Homo- and hetero-oligomerization of ammonium transporter-1  $\text{NH}_4^{+}$  uniporters. *Journal of Biological Chemistry* 278: 45603–45610.
- Luxova M. 1988. The participation of the primary maize root in the assimilation of  $\text{NH}_4^{+}$  ions. *Plant and Soil* 111: 187–189.
- Ma B, Yin CC, He SJ, Lu X, Zhang WK, Lu TG, Chen SY, Zhang JS. 2014. Ethylene-induced inhibition of root growth requires abscisic acid function in rice (*Oryza sativa* L.) seedlings. *PLoS Genetics* 10: e1004701.
- Meguro R, Asano Y, Odagiri S, Li C, Iwatsuki H, Shoumura K. 2007. Nonheme-iron histochemistry for light and electron microscopy: a historical, theoretical and technical review. *Archive of Histology and Cytology* 70: 1–19.
- Muller J, Toev T, Heisters M, Teller J, Moore KL, Hause G, Dinesh DC, Burstenbinder K, Abel S. 2015. Iron-dependent callose deposition adjusts root meristem maintenance to phosphate availability. *Developmental Cell* 33: 216–230.
- Neill SJ, Desikan R, Hancock JT. 2003. Nitric oxide signalling in plants. *New Phytologist* 159: 11–35.
- Onaga G, Dramé KN, Ismail AM. 2016. Understanding the regulation of iron nutrition: can it contribute to improving iron toxicity tolerance in rice? *Functional Plant Biology* 43: 709–726.
- Pagnussat GC, Simontacchi M, Puntarulo S, Lamattina L. 2002. Nitric oxide is required for root organogenesis. *Plant Physiology* 129: 954–956.
- Peng XX, Yamauchi M. 1993. Ethylene production in rice bronzing leaves induced by ferrous iron. *Plant and Soil* 149: 227–234.
- Peto A, Lehotai N, Feigl G, Tugyi N, Ordog A, Gemes K, Tari I, Erdei L, Kolbert Z. 2013. Nitric oxide contributes to copper tolerance by influencing ROS metabolism in *Arabidopsis*. *Plant Cell Report* 32: 1913–1923.
- Pottosin I, Dobrovinskaya O. 2014. Non-selective cation channels in plasma and vacuolar membranes and their contribution to  $\text{K}^{+}$  transport. *Journal of Plant Physiology* 171: 732–742.
- Reyt G, Boudouf S, Boucherez J, Gaymard F, Briat JF. 2015. Iron and ferritin dependent ROS distribution impact *Arabidopsis* root system architecture. *Molecular Plant* 8: 439–453.
- Roschttardtztz H, Conejero G, Curie C, Mari S. 2009. Identification of the endodermal vacuole as the iron storage compartment in the *Arabidopsis* embryo. *Plant Physiology* 151: 1329–1338.
- Shabala L, Zhang JY, Pottosin I, Bose J, Zhu M, Fuglsang AT, Velarde-Buendia A, Massart A, Hill CB, Roessner U *et al.* 2016. Cell-type-specific  $\text{H}^{+}$ -ATPase activity in root tissues enables  $\text{K}^{+}$  retention and mediates acclimation of barley (*Hordeum vulgare*) to salinity stress. *Plant Physiology* 172: 2445–2458.
- Shabala S, Demidchik V, Shabala L, Cuin TA, Smith SJ, Miller AJ, Davies JM, Newman IA. 2006. Extracellular  $\text{Ca}^{2+}$  ameliorates NaCl-induced  $\text{K}^{+}$  loss from *Arabidopsis* root and leaf cells by controlling plasma membrane  $\text{K}^{+}$ -permeable channels. *Plant Physiology* 141: 1653–1665.
- Shi HZ, Xiong LM, Stevenson B, Lu T, Zhu JK. 2002. The *Arabidopsis* salt overly sensitive 4 mutants uncover a critical role for vitamin B6 in plant salt tolerance. *Plant Cell* 14: 575–588.
- Simontacchi M, Galatro A, Ramos-Artuso FE, Santa-María G. 2015. Plant survival in a changing environment: the role of nitric oxide in plant responses to abiotic stress. *Frontiers in Plant Science* 6: 977.
- Song XG, She XP, Wang J, Sun YC. 2011. Ethylene inhibits darkness-induced stomatal closure by scavenging nitric oxide in guard cells of *Vicia faba*. *Functional Plant Biology* 38: 767–777.
- Strader LC, Chen GL, Bartel B. 2010. Ethylene directs auxin to control root cell expansion. *Plant Journal* 64: 874–884.
- Sun CL, Lu LL, Liu LJ, Liu WJ, Yu Y, Liu XX, Hu Y, Jin CW, Lin XY. 2014. Nitrate reductase-mediated early nitric oxide burst alleviates oxidative damage induced by aluminum through enhancement of antioxidant defenses in roots of wheat (*Triticum aestivum*). *New Phytologist* 201: 1240–1250.

- Szczerba MW, Britto DT, Kronzucker HJ. 2009.  $K^+$  transport in plants: physiology and molecular biology. *Journal of Plant Physiology* 166: 447–466.
- Teerawanichpan P, Hoffman T, Ashe P, Datla R, Selvarai G. 2007. Investigations of combinations of mutations in the jellyfish green fluorescent protein (GFP) that afford brighter fluorescence, and use of a version (VisGreen) in plant, bacterial, and animal cells. *Biochimica et Biophysica Acta* 1770: 1360–1368.
- Tian QY, Sun DH, Zhao MG, Zhang WH. 2007. Inhibition of nitric oxide synthase (NOS) underlies aluminum-induced inhibition of root elongation in *Hibiscus moscheutos*. *New Phytologist* 174: 322–331.
- Touraine B, Briat JF, Gaymard F. 2012. GSH threshold requirement for NO-mediated expression of the *Arabidopsis* AtFer1 ferritin gene in response to iron. *FEBS Letters* 586: 880–883.
- Wang F, Chen ZH, Liu X, Colmer TD, Zhou M, Shabala S. 2016. Tissue-specific root ion profiling reveals essential roles for the CAX and ACA calcium transport systems for hypoxia response in *Arabidopsis*. *Journal of Experimental Botany* 67: 3747–3762.
- Wang KLC, Yoshida H, Lurin C, Ecker JR. 2004. Regulation of ethylene gas biosynthesis by the *Arabidopsis* ETO1 protein. *Nature* 428: 945–950.
- Wang L, Guo YJ, Jia LX, Chu HY, Cheng KM, Wu D, Zhao LQ. 2014. Hydrogen peroxide acts upstream of nitric oxide in the heat shock pathway in *Arabidopsis* seedlings. *Plant Physiology* 164: 2184–2196.
- Ward JT, Lahner B, Yakubova E, Salt DE, Raghothama KG. 2008. The effect of iron on the primary root elongation of *Arabidopsis* during phosphate deficiency. *Plant Physiology* 147: 1181–1191.
- Weigel D, Glazebrook J. 2002. How to study gene expression. In: Weigel D, Glazebrook J, eds. *Arabidopsis: a laboratory manual*. New York, NY, USA: Cold Spring Harbor Laboratory Press, 243–245.
- Wheeler BD, Al-Farraj MM, Cook RED. 1985. Iron toxicity to plants in base-rich wetlands: comparative effects on the distribution and growth of *Epilobium hirsutum* L. and *Funcus subnodulosus* schrank. *New Phytologist* 100: 653–669.
- Xia J, Kong D, Xue S, Tian W, Li N, Bao F, Hu Y, Du J, Wang Y, Pan XJ *et al.* 2014. Nitric oxide negatively regulates AKT1-mediated potassium uptake through modulating vitamin B6 homeostasis in *Arabidopsis*. *Proceedings of the National Academy of Sciences, USA* 111: 16196–16201.
- Xiong J, Fu G, Tao L, Zhu C. 2010. Roles of nitric oxide in alleviating heavy metal toxicity in plants. *Archives of Biochemistry and Biophysics* 497: 13–20.
- Xu J, Yin HX, Li YL, Liu XJ. 2010. Nitric oxide is associated with long-term zinc tolerance in *Solanum nigrum*. *Plant Physiology* 154: 1319–1334.
- Yang ZB, Geng X, He C, Zhang F, Wang R, Horst WJ, Ding ZJ. 2014. TAA1-regulated local auxin biosynthesis in the root-apex transition zone mediates the aluminum-induced inhibition of root growth in *Arabidopsis*. *Plant Cell* 26: 2889–2904.
- Yu SP. 2003. Regulation and critical role of potassium homeostasis in apoptosis. *Progress in Neurobiology* 70: 363–386.
- Yuan HM, Huang X. 2016. Inhibition of root meristem growth by cadmium involves nitric oxide-mediated repression of auxin accumulation and signalling in *Arabidopsis*. *Plant, Cell & Environment* 39: 120–135.
- Yuan HM, Xu HH, Liu WC, Lu YT. 2013. Copper regulates primary root elongation through PIN1-mediated auxin redistribution. *Plant Cell & Physiology* 54: 766–778.
- Zepeda-Jazo I, Velarde-Buendía AM, Enríquez-Figueroa R, Bose J, Shabala S, MunizMurguía J, Pottosin I. 2011. Polyamines interact with hydroxyl radicals in activating  $Ca^{2+}$  and  $K^+$  transport across the root epidermal plasma membranes. *Plant Physiology* 157: 2167–2180.
- Zhang Y, Wang YP, Liu P, Song JM, Xu GD, Zheng GH. 2012. Effect of toxic  $Fe^{2+}$  level on the biological characteristics of rice root border cell. *Russian Journal of Plant Physiology* 59: 766–771.
- Zhang Y, Zheng GH, Liu P, Song JM, Xu GD, Cai MZ. 2011. Morphological and physiological responses of root tip cells to  $Fe^{2+}$  toxicity in rice. *Acta Physiologiae Plantarum* 33: 683–689.
- Zhou Y, Xu XY, Chen LQ, Yang JL, Zheng SJ. 2012. Nitric oxide exacerbates Al-induced inhibition of root elongation in rice bean by affecting cell wall and plasma membrane properties. *Phytochemistry* 76: 46–51.

## Supporting Information

Additional Supporting Information may be found online in the Supporting Information tab for this article:

**Fig. S1** Schematic diagram of the experimental setup for the application of excess Fe to the root tip zone.

**Fig. S2** Effects of excess Fe on root Fe staining (Perls staining) in control and in seedlings treated with excess Fe.

**Fig. S3** Effects of localized low  $K^+$  supply on the root growth of *Arabidopsis*.

**Fig. S4** Effects of excess Fe on root tip zone Na, Ca and Mg levels in *Arabidopsis*.

**Fig. S5** Effects of  $Gd^{3+}$  on Fe-inhibited root growth and effects of excess Fe on the root growth of *gork1* mutants.

**Fig. S6** Effects of  $K^+$  on root growth, net plasma membrane  $K^+$  fluxes, K content and cell viability in the root tip zone under Fe excess.

**Fig. S7** Effects of NG-nitro-L-arginine methyl ester (L-NAME) and NG-monomethyl-L-arginine (L-NMME) on the primary root growth of *Arabidopsis*.

**Fig. S8** Effects of excess Fe on primary root growth in *Arabidopsis Col-0* and *gsnor1* mutant.

**Fig. S9** Effects of Fe-citrate and K-citrate on primary root growth in *Arabidopsis Col-0* and *nox1* mutant.

**Fig. S10** Effects of Cu stress on root growth of *Col-0* and *nox1*.

**Fig. S11** Effects of auxin on excess Fe-mediated primary root growth inhibition in *Arabidopsis*.

**Fig. S12** Effects of excess Fe on the production of reactive oxygen species (ROS) in roots of *Arabidopsis Col-0* and *nox1* plants.

**Fig. S13** Effects of NO on net plasma membrane  $K^+$  fluxes in the root tip zone under control conditions.

**Fig. S14** Effects of  $Gd^{3+}$  on the NO level of the *Col-0* root tip zone.

**Fig. S15** Effects of excess Fe on cell death of the *Col-0* and *nox1* root tip zone.

**Fig. S16** Effects of NO on  $K^+$  alleviation of primary root growth inhibition under excess Fe.

**Fig. S17** Effects of excess Fe on the activity of *EBS:GUS* in *Arabidopsis* root tissue.

**Fig. S18** Effects of the NO donor sodium nitroprusside (SNP) on the activity of *AtACS7:GUS* in *Arabidopsis* root tissue.

**Table S1** Genetic loci of the *Arabidopsis thaliana* mutants used in this study

Please note: Wiley Blackwell are not responsible for the content or functionality of any Supporting Information supplied by the authors. Any queries (other than missing material) should be directed to the *New Phytologist* Central Office.



### About New Phytologist

- *New Phytologist* is an electronic (online-only) journal owned by the New Phytologist Trust, a **not-for-profit organization** dedicated to the promotion of plant science, facilitating projects from symposia to free access for our Tansley reviews and Tansley insights.
- Regular papers, Letters, Research reviews, Rapid reports and both Modelling/Theory and Methods papers are encouraged. We are committed to rapid processing, from online submission through to publication 'as ready' via *Early View* – our average time to decision is <26 days. There are **no page or colour charges** and a PDF version will be provided for each article.
- The journal is available online at Wiley Online Library. Visit **www.newphytologist.com** to search the articles and register for table of contents email alerts.
- If you have any questions, do get in touch with Central Office (np-centraloffice@lancaster.ac.uk) or, if it is more convenient, our USA Office (np-usaoffice@lancaster.ac.uk)
- For submission instructions, subscription and all the latest information visit **www.newphytologist.com**